


6-2018

DEFINING THE RADIORESPONSE OF MOSSY CELLS

Devon Ivy
California State University, San Bernardino

Follow this and additional works at: <https://scholarworks.lib.csusb.edu/etd>

 Part of the [Behavioral Neurobiology Commons](#), [Biological Phenomena](#), [Cell Phenomena](#), and [Immunity Commons](#), [Medical Cell Biology Commons](#), [Medical Molecular Biology Commons](#), [Medical Neurobiology Commons](#), [Neurosciences Commons](#), [Other Medical Sciences Commons](#), [Other Pharmacology](#), [Toxicology and Environmental Health Commons](#), and the [Radiology Commons](#)

Recommended Citation

Ivy, Devon, "DEFINING THE RADIORESPONSE OF MOSSY CELLS" (2018). *Electronic Theses, Projects, and Dissertations*. 633.
<https://scholarworks.lib.csusb.edu/etd/633>

This Thesis is brought to you for free and open access by the Office of Graduate Studies at CSUSB ScholarWorks. It has been accepted for inclusion in Electronic Theses, Projects, and Dissertations by an authorized administrator of CSUSB ScholarWorks. For more information, please contact scholarworks@csusb.edu.

DEFINING THE RADIORESPONSE OF MOSSY CELLS

A Thesis
Presented to the
Faculty of
California State University,
San Bernardino

In Partial Fulfillment
of the Requirements for the Degree
Master of Science
in
Biology

by
Devon Ivy
June 2018

DEFINING THE RADIORESPONSE OF MOSSY CELLS

A Thesis
Presented to the
Faculty of
California State University,
San Bernardino

by
Devon Ivy
June 2018
Approved by:

Nicole Bournias-Vardiabasis, PhD., Committee Chair, Biology

Jeffrey Thompson, PhD., Committee Member, Biology

Charles Limoli, PhD., University of California, Irvine, Committee Member,
Radiation Oncology

© 2018 Devon Ivy

ABSTRACT

Clinical radiotherapy is used to treat a variety of brain tumors within the central nervous system. While effective, it can result in progressive and debilitating cognitive impairment that can diminish quality of life. These impairments have been linked to hippocampal dysfunction and corresponding deficits in spatial learning and memory. Mossy cells are a major population of excitatory neurons located within the dentate hilus and highly involved in hippocampal circuitry. They play critical roles in spatial navigation, neurogenesis, memory, and are particularly vulnerable to a variety of neurotoxic insults. However, their sensitivity to ionizing radiation has yet to be investigated in detail. I hypothesize that mossy cells are critical targets for ionizing radiation, whereby damage to these targets contributes to the mechanisms associated with radiation-induced hippocampal dysfunction.

To test this idea, wild-type mice were exposed to clinically relevant doses of cranial x-ray irradiation and their hippocampi were examined 1 month and 3 months post treatment. A significant decline in both the number of mossy cells and their activity were observed. In addition, dentate granular cells demonstrated reduced levels of activity, as well as reduced proliferation within the subgranular zone. A second cohort of mice was introduced to a novel environment in order to induce the expression of immediate early genes. Analysis of *c-Fos* mRNA yielded a significant increase in control but not irradiated animals, suggesting that radiotherapy impaired immediate early gene expression and resultant functional

behavioral outcomes. These findings support the proposition that radiation-induced damage to mossy cells contributes to hippocampal deficiencies which result in cognitive dysfunction.

ACKNOWLEDGEMENTS

This thesis could not have happened if it were not for the opportunities granted by so many people. A special thank you to Dr. Bournias-Vardiabasis who saw potential, and graciously offered me the opportunity to be a part the most meaningful experience of my academic career as a fellow of the California Institute of Regenerative Medicine's Bridges program. To the California Institute of Regenerative Medicine - the Bridge's program shapes the future's scientists; it has defined my life and career, as well as so many others like me. The opportunity provided to students through this program has no equal, and I hope it continues for years to come.

Tremendous gratitude goes to Dr. Limoli for generously inviting me into his lab and being an incredible mentor. Your philosophy towards research marked an impact on me, and what I learned from you will transcend beyond this work and influence the rest of my career. Thank you to Dr. Thompson for providing such interest and useful feedback for guiding my thesis work. Thank you to Dr. Parihar who was an instrumental guiding force for my research. This thesis truly could not have been done without you. Thank you to Dr. Acharya, Dr. Baulch, Mr. Geidzinski and everyone in the Limoli lab that assisted in so many ways.

TABLE OF CONTENTS

ABSTRACT	iii
ACKNOWLEDGEMENTS.....	v
LIST OF TABLES	ix
LIST OF FIGURES	x
CHAPTER ONE: INTRODUCTION	
Brain Cancer.....	1
Radiation Therapy and Radiation Exposure	1
Radiation-Induced Cognitive Dysfunction	2
CHAPTER TWO: LITERATURE REVIEW	
Hippocampus and Subfield Anatomy.....	4
<i>Cornu Ammonis</i>	5
<i>Subiculum</i>	7
<i>Dentate Gyrus</i> and Cellular Organization.....	7
Circuitry in the Hippocampus	9
Neurogenesis.....	10
Hippocampal Plasticity	10
Deleterious Effect of Radiation on the Hippocampus.....	11
Treatment Options	13
Mossy Cells	14
Function	14
Mossy Cells and Neurogenesis.....	15
Vulnerability	16

Hypothesis	17
Aim 1: Mossy Cell Quantification.....	18
Aim 2: Activity Loss	18
Aim 3: Correlations with Neurogenesis	19
Aim 4: Epigenetic Regulation of Immediate Early Genes	19

CHAPTER THREE: MATERIALS AND METHODS

Project Overview	20
Stage 1: Molecular Analysis.....	20
Stage 2: Novelty and Memory Induction	20
Mouse Model	21
Radiation Treatment	21
0 Gray Control Cohorts	22
9 Gray Acute Cohorts.....	22
26 Gray Fractionated Cohorts	23
BrdU Labeling	23
Perfusion.....	24
Sectioning	24
Immunohistochemistry	25
Stereology.....	26
Novel Exploration for <i>c-Fos</i> Induction	27
Quantitative Real-Time PCR.....	27

CHAPTER FOUR: RESULTS

Absence of Ectopic Dentate Granule Cells	29
Stereological Quantification of Mossy Cells	29

One-Month Post Irradiation	29
Three Months Post Irradiation	30
Activity of Mossy Cells	33
One-Month Post Irradiation	33
Three Months Post Irradiation	33
Activity of Granule Cells	35
One-Month Post Irradiation	36
Three Months Post Irradiation	36
Neurogenesis	38
One-Month Post Irradiation	38
Three months Post irradiation	39
<i>C-Fos</i> Induction in Response to Spatial Novelty	41
CHAPTER FIVE: DISCUSSION	
Mossy Cell Loss Following Clinical Radiotherapy	44
Mossy Cell Inactivity and Memory Impairment	45
Mossy Cells and Neurogenesis	46
Epigenetic Regulation of <i>c-Fos</i>	47
APPENDIX A: ANTIBODIES	49
APPENDIX B: IMMUNOHISTOCHEMICAL PROTOCOLS	51
REFERENCES	58

LIST OF TABLES

Table 1. Forward and reverse primers used for RT-qPCR.	28
-------------------------------------------------------------	----

LIST OF FIGURES

Figure 1. Illustration of the hippocampus within a human brain.....	4
Figure 2. Mouse hippocampus from the coronal plane.....	6
Figure 3. Visualization of the trisynaptic circuit within the hippocampus, viewed from the sagittal plane.....	9
Figure 4. Lack of GluR2/3 (red) and Prox1 (green) colocalization within the hippocampus at 1 month (A-C) and 3 months (D-F) post-therapy.	31
Figure 5. Stereological quantification of hilar mossy cells at 1 month (A-D) and 3 months (E-G) post radiotherapy.	32
Figure 6. Immunofluorescent staining of mossy cells (red, GluR2/3) and <i>c-Fos</i> (green) at 1 month (A-C) and 3 months (D-F) post radiotherapy..	34
Figure 7. The proportion of mossy cells expressing <i>c-Fos</i> at 1 month (A) and 3 months (B) post radiotherapy.	35
Figure 8. Immunofluorescent stains of granule cells expressing <i>c-Fos</i> at 1-month (A-C) and 3 months (D-F) post radiotherapy.....	37
Figure 9. Quantification of the proportion of granule cells expressing <i>c-Fos</i> at 1 month (A) and 3 months (B) post radiotherapy.	38
Figure 10. Immunofluorescent staining of granule cells labeled with BrdU at 1 month (A-C) and 3 months (D-F) post radiotherapy.	40
Figure 11. Quantification of the number of BrdU labeled granule cells at 1 month (A) and 3 months (B) post radiotherapy.....	41
Figure 12. RT-qPCR results for <i>c-Fos</i> mRNA levels in the novel exploration experiment.....	43

CHAPTER ONE

INTRODUCTION

Brain Cancer

Brain tumors are benign and malignant uncontrolled growths of cells within the brain. They are more common among young and old and are the leading cancer that causes death in children under 14 making it more deadly than acute lymphoblastic leukemia ("Brain Tumor Statistics", 2017). Over 700,000 Americans are currently living with brain cancer and is projected to take 17,000 lives this year ("Brain Tumor Statistics", 2017). Due to the cancer residing in the brain, the plausibility of causing cerebral edema and intracranial pressure is significant and can result in dramatic and permanent changes to a person's psychological and physiological functionality. Some issues induced by these tumors include blurred vision, hearing loss, memory loss, headaches, seizures, and changes in personality ("Brain Tumor", 2017). There are options when it comes to treating brain cancer, and often these methods are used in synergy. The most frequent treatments include surgical excision, chemotherapy, and radiation therapy.

Radiation Therapy and Radiation Exposure

Administering ionizing radiation is a common medical procedure that has a variety of uses from tissue imaging to therapeutic treatments. With regard to treating cancer, the goal of using radiation is to eradicate tumors and to stop their

growth. The type of radiation and dosage varies with respect to application and the individual need of each patient. Many sources of radiation exist for medical purposes, but the most common forms are x-rays and γ -rays (photon radiation), and to a lesser extent charged particles (α , β , protons). Radiation can be administered externally usually from a linear accelerator and through brachytherapy where a radioactive material is deposited into a tissue. Ionizing radiation works to kill cancer by directly damaging DNA beyond replicative ability or damaging cells through the formation of reactive oxygen species ("Radiation Therapy for Cancer", 2017). Radiation treatment however is widely known to have serious deleterious effects on healthy normal cells and their activity and can cause long term complications in patients.

Radiation-Induced Cognitive Dysfunction

One of the latent effects of cranial radiation treatment is the development of cognitive impairment, especially in young children (Reimers et al., 2002; Edelstein et al., 2011). Patients can begin to have difficulty navigating, processing spatial information, and develop issues in learning and memory. These negative effects can initially be seen a few days after treatment and grow more severe over time; the late-onset radiation damage is believed to be what causes deficits in learning and memory (Douw et al., 2009). A dose-response effect exists in the development of radiation-induced cognitive dysfunction, with the higher doses displaying a stronger decline (Zhang et al., 2011). All of these

mentioned processes are dependent on proper hippocampal function (Bird and Burgess, 2008; Yuan et al., 2015).

CHAPTER TWO

LITERATURE REVIEW

Hippocampus and Subfield Anatomy

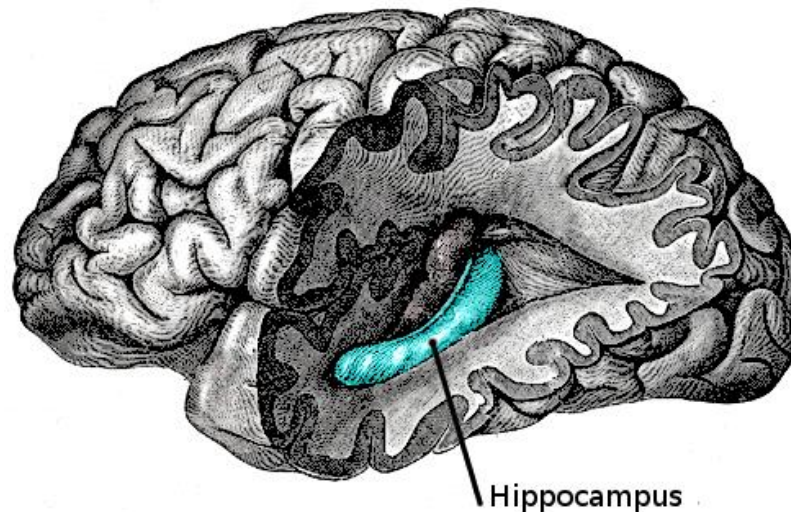


Figure 1. Illustration of the hippocampus within a human brain. By H. Gray, 1918, *Anatomy of the Human Body*. Retrieved from <https://upload.wikimedia.org/wikipedia/commons/2/2e/Gray739-emphasizing-hippocampus.png>. Public domain.

Named for its seahorse like appearance, this component of the limbic system is widely involved in learning, long term memory, and spatial navigation. Each cerebral hemisphere of the brain contains a hippocampus, which lies in the medial temporal lobe underneath the cerebral cortex. There is some ambiguity when defining regions of the hippocampus, though definitive parts include the cornu ammonis, dentate gyrus, and subiculum.

Cornu Ammonis

The cornu ammonis, abbreviated as CA, forms the region between subiculum and dentate gyrus. The cornu ammonis can be subdivided into different regions: CA1 through CA3 (and occasionally the CA4 mentioned below). Each region of the cornu ammonis primarily contains interneurons known as pyramidal cells, and the different regions help define the general circuitry within the hippocampus.

The CA1 is the region of output for the hippocampus. Synapses are received in this region from the CA3, and some input arrives from the layer III of the entorhinal cortex. Fear extinction testing shows the CA1 is directly responsible for the retrieval of contextual memory (Ji and Maren, 2008). Lying between the CA1 and CA3 regions is the CA2. The CA2 is small in size and is not involved in the predominant circuitry of the hippocampus – it receives some direct input from the entorhinal cortex. The CA2 is important for conspecific social memory (remembering an individual of the same species), shown through social behavior testing in mice (Hitti and Siegelbaum, 2014). The CA3 receives input from mossy fibers of granule cells located within the dentate gyrus, in addition to direct input from layer II of the entorhinal cortex itself. Some axons from CA3 pyramidal cells project backwards towards the entorhinal cortex while others project into the hilus, but most project towards the CA1 and CA2 via axons known as Schaffer collaterals. These axons are a key component in memory

formation and activity-dependent plasticity of the hippocampus (Vago and Kesner, 2008).

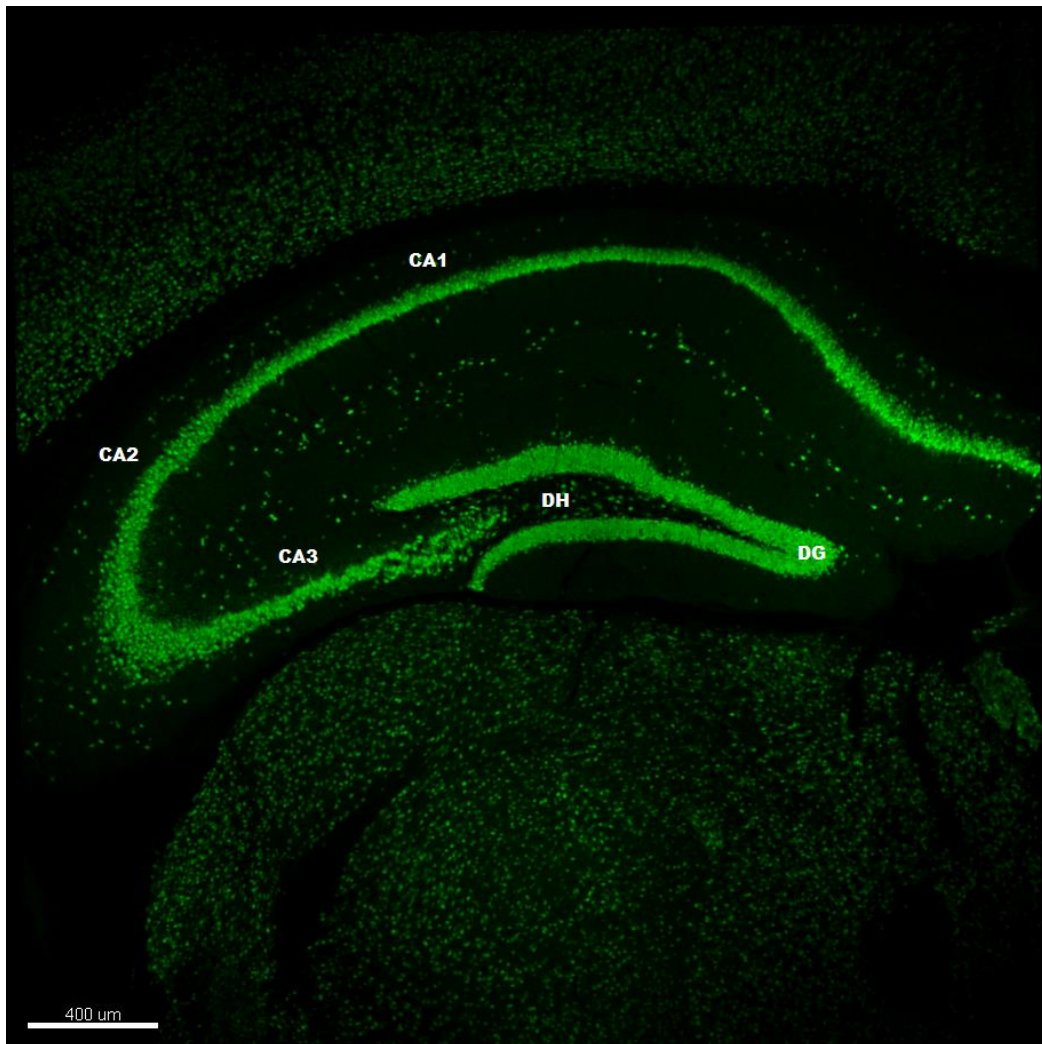


Figure 2. Mouse hippocampus from the coronal plane. Tissue immunofluorescent stained for NeuN. DH Dentate Hilus, DG Dentate Gyrus, CA3 Cornu Ammonis 3, CA2 Cornu Ammonis 2, CA1 Cornu Ammonis 1.

Subiculum

The subiculum is the most inferior part of the hippocampus and physically separates the entorhinal cortex from the hippocampus. It is a highly active region where most input leaving the hippocampus passes through. The neurons in this tissue send synapses to various parts of the brain including the amygdala, the hypothalamus, and the prefrontal cortex. The subiculum is also involved in addictive behaviors (Martin-Fardon et al., 2007).

Dentate Gyrus and Cellular Organization

Perhaps the most interesting and most studied structure of the hippocampus is the dentate gyrus. The dentate gyrus is the location in which new memories are formed and is associated with learning, stress, anxiety, and depression. It also receives incoming signals from the entorhinal cortex. Within the dentate gyrus there are four layers: the inner and outer molecular layers, the granule cell layer, and the dentate hilus.

The granule cell layer is the principle cell layer of the dentate gyrus. Granule cells are highly involved in learning (Rosi et al., 2008, Guzowski et al., 1999) and are critical for forming memories through pattern separation and pattern completion (Nakashiba et al., 2012). They have long unmyelinated axons known as mossy fibers which project into the dentate hilus towards the CA3 region and synapse with CA3 pyramidal neurons. They also synapse with mossy cells and other interneurons within the dentate hilus (Henze et al., 2000). Granule cells are primarily glutamatergic but also communicate via neurotransmitter such

as dynorphins and enkephalins (McGinty et al., 1983). The layer of cells forming the border between the dentate hilus and the granule cell layer is known as the subgranular zone, which is one of the regions of postnatal neurogenesis in the mammalian brain (Cameron and McKay, 2001).

The dentate hilus is sometimes referred to as the CA4, as it contains interneurons that regulate input into the CA3. There are a variety of these interneurons in the dentate hilus, the majority of which are inhibitory. The only native excitatory entity in this region is known as a mossy cell. There can be the occasional ectopic granule cell, which can escape from the granule cell layer under deleterious conditions (Scharfman et al., 2006). Interneurons here greatly regulate the synaptic activity of granule cells. Much input leaves the dentate gyrus via the dentate hilus towards the CA3. The dentate hilus plays an active role in mood, having influences on stress, depression, and anxiety.

The molecular layer of the dentate gyrus consists primarily of dendrites belonging to granule cells. The molecular layers are where afferent input from the entorhinal cortex arrives in the dentate gyrus. Here, synapses with the dendrites of granule cells bring the input into the hippocampus along the pathway known as the perforant pathway, marking the beginning of the trisynaptic circuit.

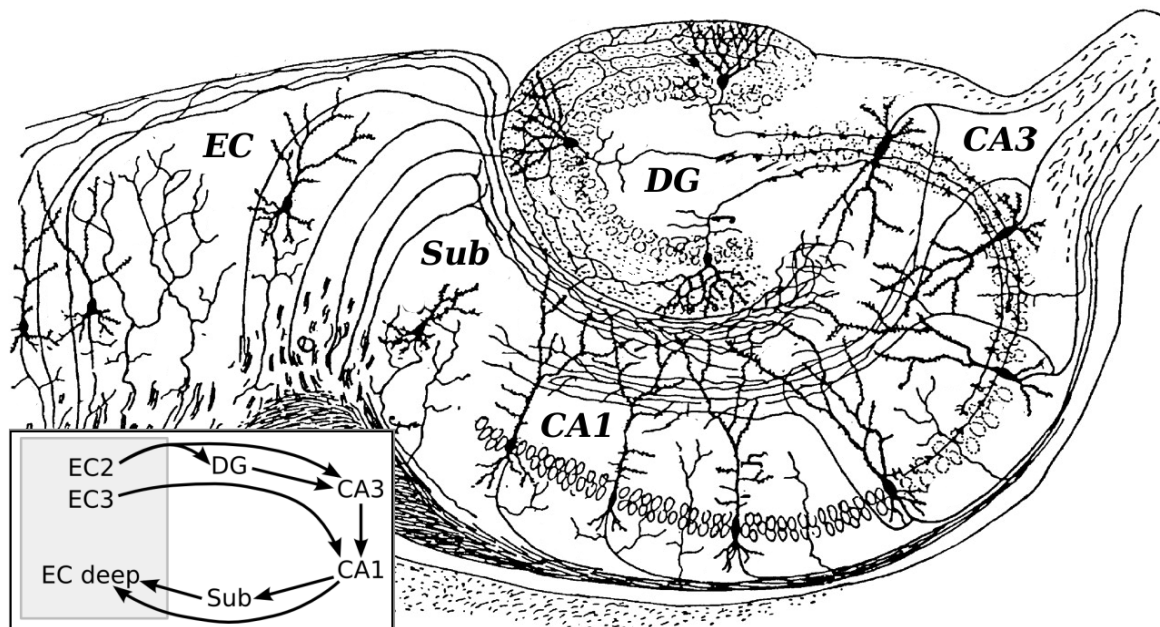


Figure 3. Visualization of the trisynaptic circuit within the hippocampus, viewed from the sagittal plane. EC Entorhinal cortex, Sub Subiculum, DG Dentate Gyrus, CA3 Cornu Ammonis 3, CA1 Cornu Ammonis 1. EC2 and EC3 refer to subsections 2 and 3 of the entorhinal cortex. By S. Ramón y Cajal, 1911, *Histologie du Système nerveux de l'Homme et des Vertèbres*, Retrieved from https://upload.wikimedia.org/wikipedia/commons/2/25/CajalHippocampus_%28modified%29.png. Public domain.

Circuitry in the Hippocampus

The primary synaptic pathway of the hippocampus is unidirectional and known as the trisynaptic circuit. Input starts from pyramidal cells within layers 1 and 2 of the entorhinal cortex and enters the dentate gyrus through synapses with granule cells in the outer molecular layer. From there, information is transmitted along the mossy fibers of granule cells to CA3 pyramidal cells. Input travels further and reaches the CA1 from the CA3 via the Schaffer collateral

pathway. Synapses leave the CA1 and either move towards layers 5 and 6 of the entorhinal cortex or into the subiculum. The trisynaptic circuit allows afferent input to reach all regions of the hippocampus. Other input from the entorhinal cortex directly travels to CA3 and CA1. Output from the hippocampus can reach the prefrontal cortex, hypothalamus, and the septal nuclei. The septal nuclei also innervate the hippocampus with choline and GABA.

Neurogenesis

The hippocampus is one of the few known regions of adult neurogenesis within the brain. The region specifically is the subgranular zone of the dentate gyrus, which is the row of cells closest to the dentate hilus. Neural stem cells in the subgranular zone are capable of self-renewal, are unspecialized, and can give rise to neurons, astrocytes, and oligodendrocytes throughout adult life. Adult born neurons must be able to migrate and functionally integrate to existing hippocampal circuitry of the dentate gyrus. Specific tasks, such as pattern separation and ability to form new memories, are associated with these newborn granule cells (Nakashiba et al., 2012). The granule cell layer can be viewed as a temporal gradient: the region closest to the dentate hilus is the youngest, and the cells at the furthest out region towards the molecular layer are the oldest.

Hippocampal Plasticity

The hippocampus has a remarkable ability to reorganize neuronal synapses throughout development and adult life. Granule cells of the dentate gyrus have a diverse synaptic arrangement, and this arrangement changes over

time with the integration of adult-born granule cells. Other cells, such as pyramidal cells, demonstrate increasing dendritic complexity with age (Seress and Ribak, 1995). Learning contributes the establishment of neuronal circuits within the dentate gyrus and CA3 due to the plasticity of the region, shown through the behaviorally expressed protein *Arc* which travels to the dendrites closest to active synapses (Rosi et al., 2008). Other proteins are involved in the dynamic activation and solidification of neural circuits, including *c-Fos* and *zif-268* (Guzowski et al., 1999). With this plasticity of neuronal circuits, the hippocampus plays an active role in responding to incoming stimuli.

Deleterious Effect of Radiation on the Hippocampus

While the mechanisms behind radiation-induced cognitive dysfunction are not completely understood, the pathogenesis is strongly associated with persistent neuroinflammation, oxidative stress, and genomic instability. The tissue response to ionizing radiation is to secrete proinflammatory cytokines and chemokines, similarly to neurodegenerative diseases such as Alzheimer's disease (Agostinho et al., 2010). Ionizing radiation produces a change in the cellular microenvironment with the associated production of these inflammatory markers by microglia and astroglia, which themselves are activated by the radiation exposure (Parihar et al., 2014; Acharya et al., 2015; Zhou et al. 2017). These chemokines are cytotoxic and cause continuing damage to hippocampal tissue.

In addition to secreting proinflammatory proteins, microglia will release reactive oxygen species in order to recruit and mobilize more inflammatory responses (Garden, 2013). The microglia damage the integrity of the blood-brain barrier, which permits the travel of peripheral immune cells to the brain; there is also a net decrease in blood flow to the hippocampus (Zhout et al., 2017). Reactive oxygen species are produced via water radiolysis from the ionizing radiation, which results in oxidative stress to cells. These reactive oxygen species reduce dendritic complexity and both the number and density of dendritic spines within the dentate gyrus in a dose-dependent manner (Parihar and Limoli, 2013, Huang et al., 2012, Rola et al., 2008).

Ionizing x-ray and space-simulated radiation can modulate gene expression within the hippocampus, a phenomenon often referred to as radiation induced genomic instability (Acharya et al., 2015; Wang et al., 2014). Many chromosomal rearrangements and mutations occur; in addition, many different genes become activated or inactive following exposure. There are two main methods of this occurring: through the methylation of DNA and through damages in the genome. A single gray of ionizing radiation provides enough energy to break 40 base-pair bonds between nucleotide base pairs; across an entire genome (3.1 billion base-pairs in humans, 2.7 billion in mice) this effect is almost insignificant and does not explain the shift in genetic expression after radiation exposure. The more likely culprit of altered gene expression is the methylation of histone cytosine residues within the hippocampus via increased activity of DNA

methyltransferase and other DNA methylating enzymes (Acharya et al., 2017; Antwi et al., 2013). Epigenetic modulation of the genome can result in dramatic differences in cellular function, structure, and activity.

Furthermore, postnatal neurogenesis is significantly halted after ionizing radiation exposure (Deng et al., 2009; Rola et al., 2004). Effects are seen in the organismal level, as animals exposed to radiation therapy demonstrate reduced performance in hippocampal dependent behavioral tasks (Parihar et al., 2014). Cranial irradiation also reduces the expression of the behaviorally induced *Arc* protein and damages plasticity of the hippocampus (Rosi et al., 2008).

Treatment Options

As therapies for brain cancer improve and survival rates for brain cancer increases, the number of patients with long term cognitive dysfunction increases. Despite scientific communities knowing about the side effects of cranial radiation treatment for nearly 30 years, no treatment exists to this day to cure this medical need. Current efforts are strongly focused on reducing neuroinflammation and promoting neurotrophic factor production through different approaches. Drugs like memantine and donepezil are under testing in both preclinical and clinical trial stages (Brown et al., 2013; Shaw et al., 2006). Exercise is suggested to be beneficial as it has been shown to reduce neuroinflammation within the hippocampus and promote neurogenesis through the secretion of neurotrophic factors (Kohman et al., 2013; Nokia et al., 2016). The most exciting and promising therapies are human neural stem cells used to rescue cognitive

function after transplantation into irradiated brains (Acharya et al., 2011; Acharya et al., 2009) and that transplanting partially differentiated neural precursors prevents the formation of teratomas. There appears to be no detrimental side effects to this therapy. Most of the neural stem cells secrete neurotrophic factors to promote brain health and that reduces inflammation and restores cognitive function rather than integrate into the hippocampal circuitry, though some do. Neural stem cell derived extracellular vesicles have also been used to restore cognitive function without the need for brain surgery as they can be administered through intravenous injections (Baulch et al., 2016).

Mossy Cells

The name mossy cell was given for the mossy-like appearance seen initially in Golgi staining. Mossy cells are excitatory interneurons exclusively located within the dentate hilus. Mossy cells are not to be confused with mossy fibers, the long unmyelinated axons originating from granule cells projecting into the CA3. The mossy cell somata are multipolar, often appearing triangular in shape.

Function

Mossy cells form a complex circuitry within the dentate hilus, but the main purpose appears to be regulation of granule cell activity. The axons project into the molecular layers of the dentate gyrus and synapse with granule cells, while their dendrites are short and rarely leave the hilus (Scharfman, 2016). A small portion of the axons synapse with CA3 pyramidal cells and hilar interneurons like

basket cells and HIPP cells (Buckmaster et al., 1996). The axons can be extraordinarily long, projecting to the contralateral hippocampus (Buckmaster et al., 1996). Synaptic input to mossy cells is primarily excitatory and from both granule cells and CA3 pyramidal cells, with some inhibitory input arriving from hilar interneurons (Scharfman, 1994). Mossy cells themselves provide direct glutamatergic excitation to granule cells, but also excite inhibitory interneurons within the dentate hilus. These inhibitory interneurons then inhibit granule cells. Mossy cells theoretically could contribute to excitation and inhibition of the same granule cell. The net effect appears to be inhibitory (Scharfman, 2016).

Mossy cells are involved in hippocampal-dependent behavioral tasks. Pattern separation is a process that separately defines afferent inputs in the dentate gyrus that have overlapping pathways and creates different outputs from similar inputs. For example, overlapping inputs from the layers 1 and 2 of the entorhinal cortex reaching the dentate gyrus that represent similar spatial and temporal settings. Mossy cells will selectively fire to separate these inputs. In vivo imaging of mossy cells in behavioral tests shows mossy cells remap these firing fields during novel foraging (Danielson, 2017). Mossy cells are also involved in spatial navigation, as the dentate gyrus is responsible for recognizing novelty in an environment (Vago and Kesner, 2008).

Mossy Cells and Neurogenesis

Not much is known about the influence mossy cells have on hippocampal neurogenesis. It was demonstrated through a mossy cell knockout line that upon

selective knock-out, pattern separation is impaired (Jinde et al., 2012). This task is strongly associated with postnatal neurogenesis (Nakashiba et al., 2012; Danielson et al., 2017; Clelland et al., 2009; Snyder et al., 2009). Mossy cells provide the first glutamatergic input onto maturing newborn granule cells at around 2 weeks of age (Chancey et al., 2014). Mossy cells have further been suggested to be important for functionally maturing adult-born granule cells through their expression of dysbindin-1C (Wang et al., 2014). In patients suffering from epileptic seizures, mossy cells are lost which simultaneously correlates with aberrant maturation and integration of newborn granule cells (Scharfman et al., 2006). While the role of mossy cells in neurogenesis is somewhat uncertain, they appear to be important for functional integration and maturation of adult-born granule cells.

Vulnerability

The most interesting phenomenon of mossy cells, and what attracted attention to them initially, is their vulnerability to a variety of insults and illnesses. In essence, when the hippocampus is under stress, mossy cell numbers are diminished. The earliest examples demonstrating vulnerability of polymorphic (dentate hilar) cells is shown in patients with temporal lobe epilepsy (TLE) (Seress et al., 2009). Here, patients that suffered from TLE had significant cell loss within the hilar region of the dentate gyrus. Decades later these cells were demonstrated to be mossy cells and HIPP (hilar interneuron perforant pathway) cells (Magloczky and Freund, 1993). In schizophrenia, mossy cells are

vulnerable because they express DNTBP1, a leading susceptibility gene often mutated in the disease (Wang et al., 2014; Falkai and Bogerts, 1986; Owen et al., 2004). DNTBP1, coding for dysbindin, is involved with hallucinations (Cheat et al., 2015). Mossy cells and possibly few other hilar interneurons express dysbindin-1C, which is necessary for mossy cell survival and for the production of autophagosomal membranes (Yuan et al., 2015). Without dysbindin-1C, the autophagic response is severely weakened and can result in cell death. Other insults, such as forebrain ischemia (hypoxia) and traumatic brain injury both result in a significant drop in number of mossy cells (Hsu and Buzsaki, 1993).

As stated earlier, mossy cells are imperative to hippocampal dependent tasks such as spatial navigation, pattern separation, and the integration and maturation of adult-born granule cells. These tasks are disrupted in those suffering from radiation-induced cognitive dysfunction. However, the effect of radiation exposure on mossy cells has not yet been studied and they could be an overlooked target that contributes to the cognitive dysfunction seen following clinical radiation treatment. This project is the first that investigates any potential impact of radiation treatment on the cellular homeostasis of mossy cells.

Hypothesis

Mossy cells are critical targets for ionizing radiation and can contribute to the mechanisms associated with radiation-induced cognitive dysfunction.

Aim 1: Mossy Cell Quantification

If mossy cells are sensitive to radiation in similar ways as the other stresses, their numbers will be reduced after radiation treatment. The number of mossy cells within the dentate hilus will be quantified via unbiased stereology. The most ubiquitous and widely accepted marker for mossy cells is the glutamate receptor, GluR2/3 (EMD Millipore #AB1506). Within the dentate hilus, mossy cells are the only glutamatergic entity aside from ectopic granule cells. Ectopic granule cells are rare and normally arise from epileptic damage to the hippocampus (Scharfman et al., 2006). Prox1, a marker of granule cells, will be used to determine if they escape to the hilus after radiation treatment and will not be quantified.

Aim 2: Activity Loss

If a portion of mossy cells remain after radiation therapy, their activity will be measured through the marker *c-Fos*. Immediate early genes (IEG) are genes that activate quickly in response to specific stimuli. *c-Fos*, an IEG, is normally expressed within the hippocampus when neurons fire action potentials in response to environmental novelty, is connected to memory formation, and is commonly accepted as a marker for an active neuron. *c-Fos* is basally expressed in mossy cells under normal housing conditions (Duffy et al., 2013, VanElzakker et al., 2008). The expression of *c-Fos* will be quantified within both mossy cells and granule cells. Granule cells will be quantified as mossy cells play important regulatory roles for them. Mossy cells will be quantified via dual staining of *c-Fos*

and GluR2/3. Granule cells will be co-stained stained for NeuN, a marker of a mature neuron, in addition to *c-Fos*.

Aim 3: Correlations with Neurogenesis

The effect of radiation therapy on neurogenesis will be measured through immunofluorescent staining of 5-bromo-2-deoxyuridine (BrdU) with NeuN. This data will correlate with the potential loss in mossy cells and mossy cell activity.

Aim 4: Epigenetic Regulation of Immediate Early Genes

C-Fos is expressed in rapid response to environmental novelty and encoding of spatial memories in mossy cells (Bui et al., 2018). If ionizing radiation is able to epigenetically regulate the expression of IEGs, then it is possible that the translation of *c-Fos* mRNA may be prevented. A separate cohort of animals will be subject to a novel spatial environment paradigm to induce the transient expression of *c-Fos*.

CHAPTER THREE

MATERIALS AND METHODS

Project Overview

Mice were cranially irradiated at clinically relevant doses followed by immunohistochemical analyses of different markers using different analytical techniques. Two different cohorts of animals were utilized, one of which was exposed to environmental novelty to induce IEG expression.

Stage 1: Molecular Analysis

36 mice will be used for immunohistochemical analyses. There were be two time points studied: 1 month and 3 months post radiation treatment. At each time point 18 mice were sacrificed to study aims 1-3.

Stage 2: Novelty and Memory Induction

24 mice were used for an immediate early gene (IEG) induction experiment. 12 animals are cage controls, 12 are experimental groups. Experimental animals were permitted to explore a novel environment with toys and sacrificed 30 minutes afterwards to preserve the transient expression of *c-Fos* induced from the behavior task. Cage controls are held without the novel exploration to establish baseline IEG levels and are sacrificed similarly.

Mouse Model

The mice and procedures used are approved according to the Institutional Animal Care and Use Committee (IACUC) of University of California, Irvine and the National Institute of Health (NIH). Male C57BL6/J mice obtained from Jackson Laboratories are being used in this study. Mice were housed in ventilated cages and fed a diet of standard mouse pellet chow and given a standard light and dark cycle of 12 hours each daily. These mice were all 8 weeks (2 months) of age at radiation treatment.

Radiation Treatment

Clinical radiation administered consisted of x-rays generated by an X-RAD 320, an x-ray irradiator manufactured by Precision X-Ray. Treatments were given head-only. A gray (Gy) of radiation is an absorbed dose of ionizing radiation measured in terms of joules per kilograms of tissue.

Clinical fractionated doses were calculated according to the biologically effective dosage (B.E.D) formula (Hall and Giaccia, 2006).

$$BED = nd \left(1 + \frac{d}{\frac{\alpha}{\beta}} \right)$$

This formula translates the total dose (nd where n is the number of doses and d is the individual dose, e.g. 8.67 Gy) administered and its relative effectiveness ($1 + d/\alpha/\beta$, where α/β is a value in which the linear and quadratic

aspects of cell survival are equivalent, specific to cell type¹. In this case, the value is 3 Gy) into the total effective dosage. The 26 Gy fractionated total dose across 3 individual doses of 8.67, when put into this formula:

$$BED = (3 \text{ fractions}) \left(8.67 \frac{\text{Gy}}{\text{fraction}} \right) \left(1 + \frac{8.67 \text{ Gy}}{3 \text{ Gy}} \right)$$

$$BED = 101.2 \text{ Gy}$$

This value is equivalent to the quantity administered to human patients undergoing radiation therapy for glioblastoma and other CNS cancers, within conservative error. Conventional human treatments consist of 30 fractions of 2 Gy, given one fraction a day for 5 days a week shown below (Hall and Giaccia, 2006).

$$BED = (30 \text{ fractions}) \left(2 \frac{\text{Gy}}{\text{fraction}} \right) \left(1 + \frac{2 \text{ Gy}}{3 \text{ Gy}} \right)$$

$$BED = 100 \text{ Gy}$$

0 Gray Control Cohorts This treatment was a sham irradiation and animals were handled and anaesthetized similarly to irradiated groups.

Stage 1. 12 mice were administered 0 grays of radiation.

Stage 2. 8 mice were administered 0 grays of radiation.

9 Gray Acute Cohorts: This treatment was done in a single dose. This is a historical dose administered to study effects of ionizing radiation.

¹ Mammalian cells *in vivo* exposed to x- and γ- rays have a survival curve in which both linear and quadratic components of cell killing are present. The linear component, αD, and the quadratic component, βD², provide an equal effect at a dose D where D = α/β (Hall & Giaccia, 2006).

Stage 1. 12 mice were administered 9 grays of radiation.

Stage 2. 8 mice were administered 9 grays of radiation.

26 Gray Fractionated Cohorts: These treatments were split up across three nonconsecutive days (i.e. Monday, Wednesday, then Friday). A fractionated radiation treatment simulates a large dose administered in a manner to lessen the damage dealt to healthy cells while permitting a large quantity of ionizing radiation delivered.

Stage 1. 12 mice were administered 26 grays of fractionated radiation (8.67 Gy three times).

Stage 2. 8 mice were administered 26 grays of fractionated radiation (8.67 Gy three times).

All mice underwent full sedation for these procedures. Isoflurane was mixed with oxygen in an enclosed chamber to anaesthetize the mice. The mice remained anaesthetized during radiation treatment and were aroused shortly afterwards. The acute dose is administered on the last day of the fractionated dose. Control mice were anaesthetized sham-irradiated each time with the fractionated cohorts.

BrdU Labeling

5-bromo-2-deoxyuridine (BrdU) is an analog to thymine that incorporates into DNA and allows for the labeling of proliferating cells. Within the hippocampus specifically, BrdU allows for the detection of adult born cells arising from the stem

cell niche within the subgranular zone. Around 1 month is required for an adult-born granule cell to reach maturity. BrdU was administered (Sigma, St. Louis, MO) via intraperitoneal injections at a concentration of 50 mg BrdU per 1 kg of subject body mass. These injections were given for 6 consecutive days 1 month before the perfusion time points. 6 mice per cohort at each time point were administered BrdU.

Perfusion

1 month after the last BrdU injection, mice were sacrificed via intracardial perfusions. All the animals scheduled for perfusion were transferred to a separate room in their housing cage covered with black bag and remained so until individual perfusion begun. Mice were deeply anaesthetized with isoflurane and remained anaesthetized while a 30 ml saline solution consisting of phosphate-buffered saline (PBS) and heparin was injected into the left ventricle. Subsequently mice were intracardially perfused by 50 ml of 4% paraformaldehyde (PFA) in PBS solution. The brains were then removed and held in a 4% paraformaldehyde fixative for 24 hours at 4°C.

Sectioning

Brains processed were held in an increasing sucrose gradient of 10%, 20%, and 30% before sectioning. Brains were cut along the coronal plane at a thickness of 30 microns using a Leica cryostat (Leica Biosystems CM1950). Afterwards, the tissue sections were held in PBS with 0.02% sodium azide as a

preservative until long term storage in a cryo buffer. Cryo buffer consists of by volume 30% ethylene glycol, 30% glycerol, 40% PBS, and 0.2% sodium azide by weight.

Immunohistochemistry

Tissue sections for immunostaining were incubated in CytoOne 24-well plates. Serial sections (2 per animal, every 20th section) of tissue are immunohistochemically stained for the different *c-Fos*, NeuN, and BrdU aims from at least 3 animals of each group. All immunohistochemical protocols can be located in Appendix B.

Quantification of mossy cells expressing *c-Fos* was done on tissues stained for *c-Fos* and GluR2/3. Dual-positive quantification will be done under confocal microscopy. Specifically, the total number of mossy cells per tissue and number of mossy cells positive for *c-Fos* were counted. The proportion of mossy cells expressing *c-Fos* per section was mathematically determined.

Quantification of granule cells expressing *c-Fos* was done on tissues stained for *c-Fos* and NeuN. The proportion of granule cells expressing *c-Fos* was determined through Imaris analysis; the number of granule cells per section is too large to count manually.

Quantification of BrdU positive granule cells was conducted on tissues stained for BrdU and NeuN. This was done manually under confocal microscopy; the total number of BrdU tagged granule cells per section was reported.

Stereology

Stereology is a method of quantifying components of a volume based from representative cross sections of the material. Stereology was performed on the number of mossy cells within the dentate hilus of 30 micrometer coronal sections of mouse brain tissue. Six sections of brain tissue will be used per animal; 18 animals were analyzed at both the 1 month and 3-month time points (108 sections of tissue per time point)². Mossy cells were visualized through a bright-field stain for GluR2/3. Every 10th section throughout the entire hippocampus was processed. Color development was through the avidin-biotin-complex method and enhanced diaminobenzidine substrate (Vector Labs); all sections were counterstained with Nuclear Fast Red (Vector Labs). Stereologic quantification was conducted using a Nikon Eclipse Ti-E microscope with a MBF CX9000 color digital camera, 100x oil-immersion (1.30NA) objective lens, a 3-axis stage, and StereoInvestigator software (MBF Biosciences, v9). The yield of GluR2/3 positive cells was conducted using the optical fractionator probe, and systematic random sampling of each section was carried out according to unbiased stereology principles. The volume connecting the two blades of the dentate gyrus and CA3 within the dentate gyrus (the dentate hilus) is the location in which quantification took place.

² One of the 26 Gy-treated mice scheduled for perfusion at 3-months post radiotherapy passed away prior to perfusion.

Novel Exploration for *c-Fos* Induction

To induce the expression of *c-Fos* in mossy cells, mice were allowed to explore freely in an open arena (8 x 3 x 10 cm) for a single 5-minute session. The open arena contained two toy objects. After the exploration period, mice were returned to their regular housing cages and sacrificed 30 minutes later via decapitation after deep sedation with isoflurane. The fresh brains were sliced in half along the sagittal plan, separating into two hemispheres. Half of the brain was frozen in OCT freezing media for immunohistochemical staining and analysis of *c-Fos* and GluR2/3. The other hemisphere was micro-dissected to remove the hippocampus, which was then snap-frozen in liquid nitrogen and stored at -80°C. These hippocampi were used to quantify the absolute levels of *c-Fos* mRNA levels via RT-qPCR. A separate cohort of animals, cage controls, did not undergo exploration in order to establish basal levels of *c-Fos* expression. These animals were transported, sacrificed, and processed identically to the exploration groups.

Quantitative Real-Time PCR

RNA was collected from hippocampi dissected from fresh brains not fixated with PFA. RNA collection was done with a Direct-zol RNA MicroPrep kit (Zymo Research) following the manufacturer's protocols. cDNA was prepared using Invitrogen's SuperScript III according to manufacturer protocols. qPCR was conducted on a BioTek plate reader following the SuperScript III protocols with the addition of SYBR Green fluorescent dye. The primers for *c-Fos* and actin

(normalization and positive control) were used. Data were reported as the absolute ratio of *c-Fos* mRNA to actin mRNA multiplied by 1000.

Table 1. Forward and reverse primers used for RT-qPCR.

Primer	Forward (5' to 3')	Reverse (5' to 3')
<i>c-Fos</i>	AGCAGCTATCTCCTGAAGAG	CAGATTGGCAATCTCAGTCTG
Actin-B	TCCTGTGGCATCCATGAAAC	TGATCTTCATTGTGCTGGGT

CHAPTER FOUR

RESULTS

Absence of Ectopic Dentate Granule Cells

Through fluorescent immunostaining for Prox1 and GluR2/3 (two sections per animal, three animals per group), no cell within the dentate hilus was found positive for both markers at 1-month (Figure 4 A-C) and 3 months (Figure 4 D-F) post irradiation in every section observed.

Stereological Quantification of Mossy Cells

Brain sections were bright-field immunostained with glutamate receptor (GluR2/3 EMD Millipore #1506) to illuminate mossy cells within dentate hilus. 6 tissues from each animal were analyzed; the mean number of mossy cells per animal was stereologically estimated following unbiased stereological principles. Representative images can be seen in Figure 5.

One-Month Post Irradiation

At 1-month post irradiation, exposure to both 9 Gy and 26 Gy of x-ray irradiation resulted in a significant decrease in the number of mossy cells compared to controls (n=6 per group, One-way ANOVA, $F=11.28$, $P=0.001$; Figure 5H). Unbiased stereological estimation yielded a 23% loss at 9 Gy and a 34% loss at 26 Gy, respectively. Bonferroni's multiple comparisons test was used post hoc and resulted in a significant difference between the means of 0 Gy and

9 Gy ($t=3.221$, $P<0.05$), 0 Gy and 26 Gy ($t=4.634$, $P<0.001$), but not between 9 Gy and 26 Gy ($t=1.414$, $P>0.05$).

Three Months Post Irradiation

Results were similar for the 3 months post irradiation analysis. A significant difference was found in both 9 Gy and 26 Gy cohorts, with stereological estimates of a 27% decrease at 9 Gy and a 26% decrease at 26 Gy compared to controls ($n=5$ per group, One-way ANOVA, $F=11.76$, $P=0.0015$; Figure 5H). Post hoc analysis with Bonferroni's multiple comparison test yielded a significant difference between 0 Gy and 9 Gy ($t=4.237$, $p<0.01$), 0 Gy and 26 Gy ($t=4.160$, $P<0.01$), but not between 9 Gy and 26 Gy ($t=0.07775$, $P>0.05$).

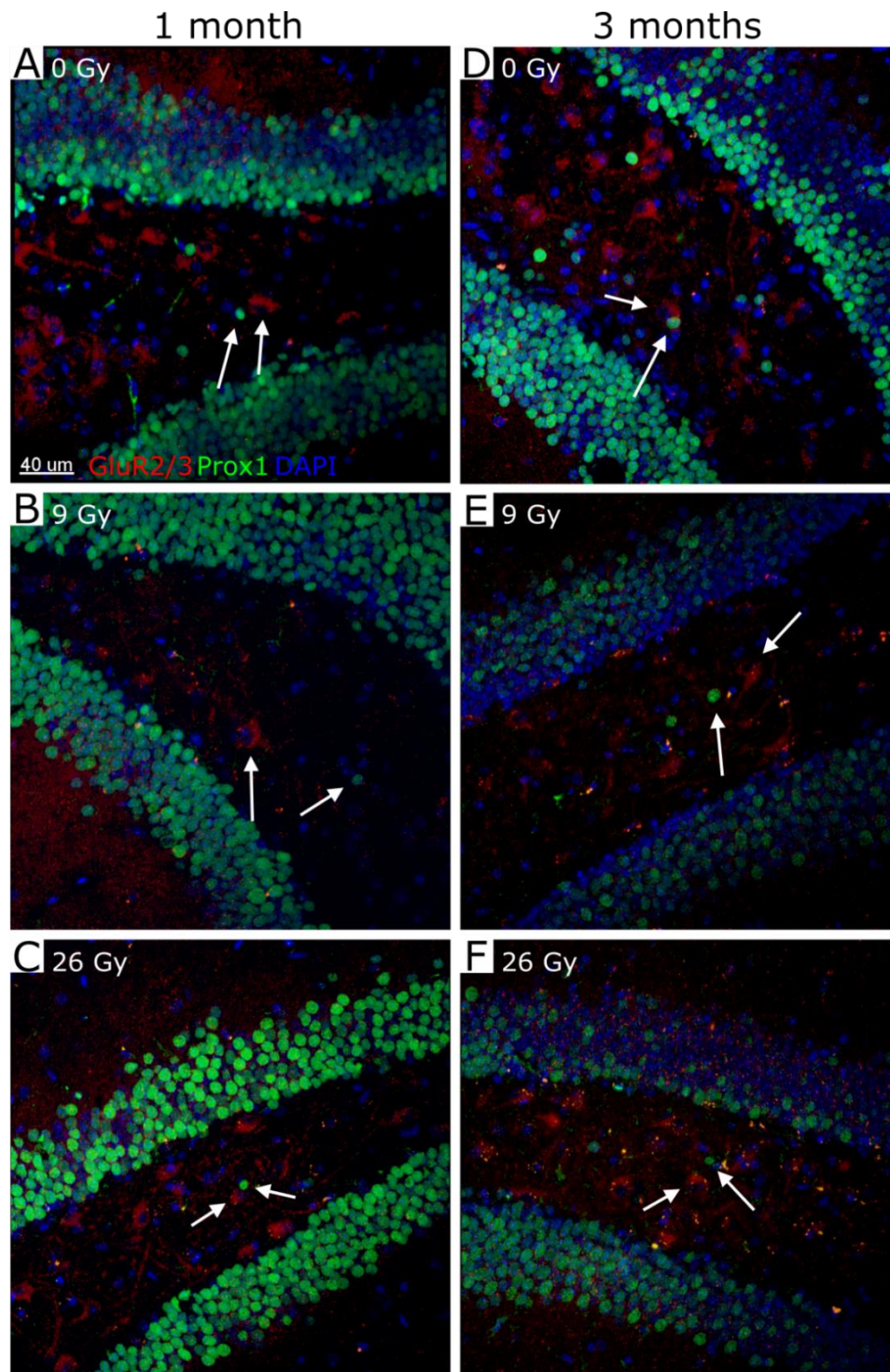


Figure 4. Lack of GluR2/3 (red) and Prox1 (green) colocalization within the hippocampus at 1-month (A-C) and 3 months (D-F) post-therapy. Arrows indicate a hilar nucleus positive for Prox1 and its closest GluR2/3 positive soma.

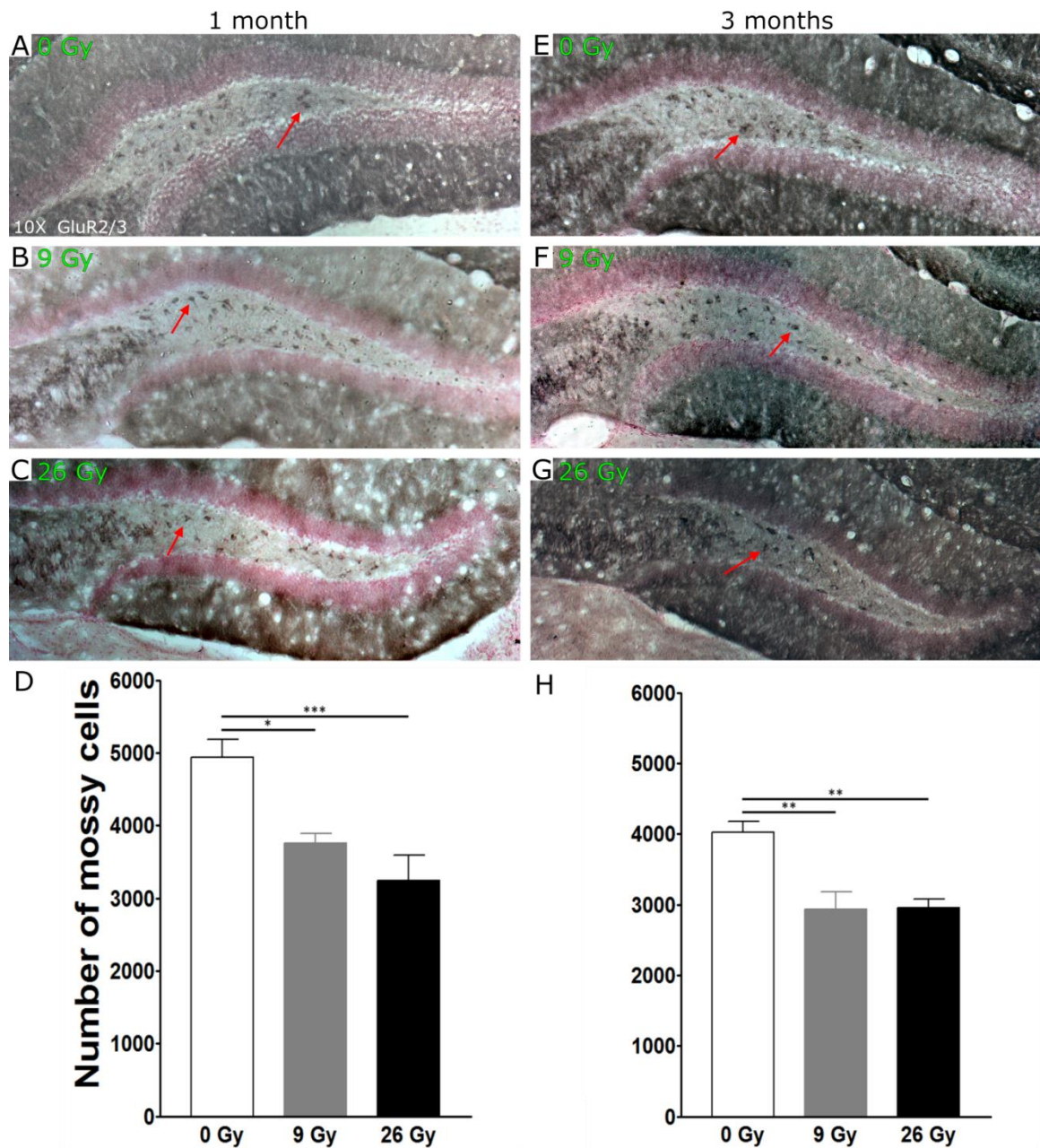


Figure 5. Stereological quantification of hilar mossy cells at 1-month (A-D) and 3 months (E-G) post radiotherapy. Stereologic estimation of the number of mossy cells at 1-month (D) and 3 months (H) post radiotherapy. Arrows indicate mossy cells. Data are expressed as mean \pm SEM. * $P < 0.05$, ** $P < 0.01$, *** $P < 0.001$; One-way ANOVA followed by Bonferroni's multiple comparison post-hoc analysis.

Activity of Mossy Cells

Measurements of activity within mossy cells were conducted through dual immunofluorescent staining of *c-Fos* (*c-Fos* [2H2] Abcam #ab208942) and glutamate receptor (GluR2/3). Representative images can be seen in Figure 6.

One-Month Post Irradiation

Analysis of two pieces of tissue per animal (n=5 animals) from similar regions of the brain (one rostral, one caudal) resulted in a significant decrease in dual-immunoreactivity among group means (One-way ANOVA, $F=8.517$, $P=0.0027$; Figure 7A). The proportions of mossy cells expressing *c-Fos* are 17.6% at 0 Gy, 8.4% at 9 Gy, and 5.4% at 26 Gy. Post hoc analysis using Bonferroni's multiple comparison test yielded a significant difference between 0 Gy and 9 Gy groups ($t=3.162$, $P<0.05$), 0 Gy and 26 Gy groups ($t=3.932$, $P<0.01$), but not between 9 Gy and 26 Gy groups ($t=1.042$, $P>0.05$).

Three Months Post Irradiation

At three months post irradiation, a similar decrease in activity levels was observed. A significant difference among group means was found (One-way ANOVA, $F=12.38$, $P=0.0002$; Figure 7B). Group means are 10.1% at 0 Gy, 5.6% at 9 Gy, and 1.6% at 26 Gy. When compared individually using Bonferroni's multiple comparison test, a significant difference was observed between the group means of 0 Gy and 9 Gy ($t=2.655$, $P<0.05$), 0 Gy and 26 Gy ($t=4.972$, $P<0.001$), but not between 9 Gy and 26 Gy ($t=2.317$, $P>0.05$).

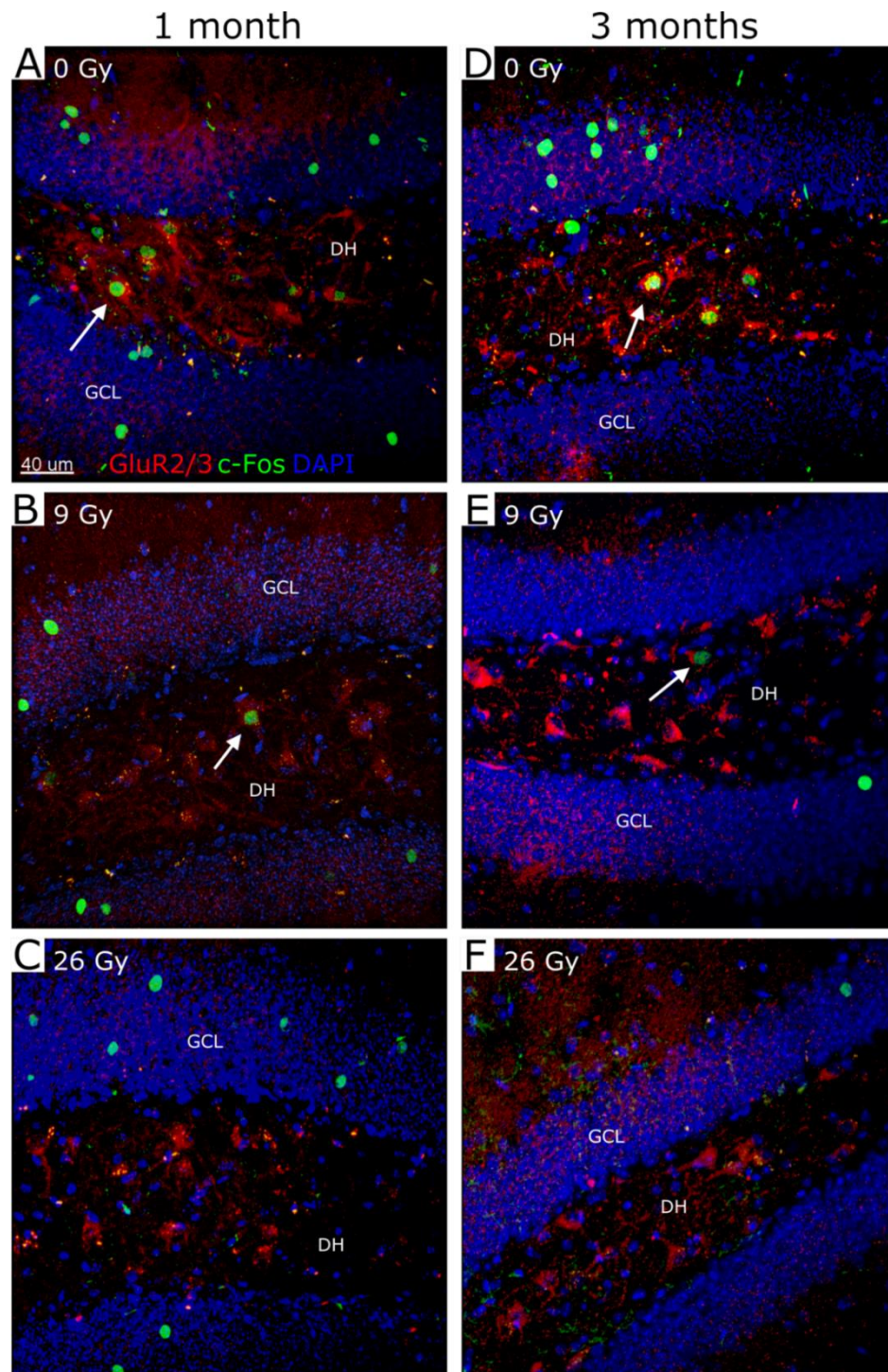


Figure 6. Immunofluorescent staining of mossy cells (red, GluR2/3) and *c-Fos* (green) at 1-month (A-C) and 3 months (D-F) post radiotherapy. Arrows indicate co-labeling of *c-Fos* and GluR2/3.

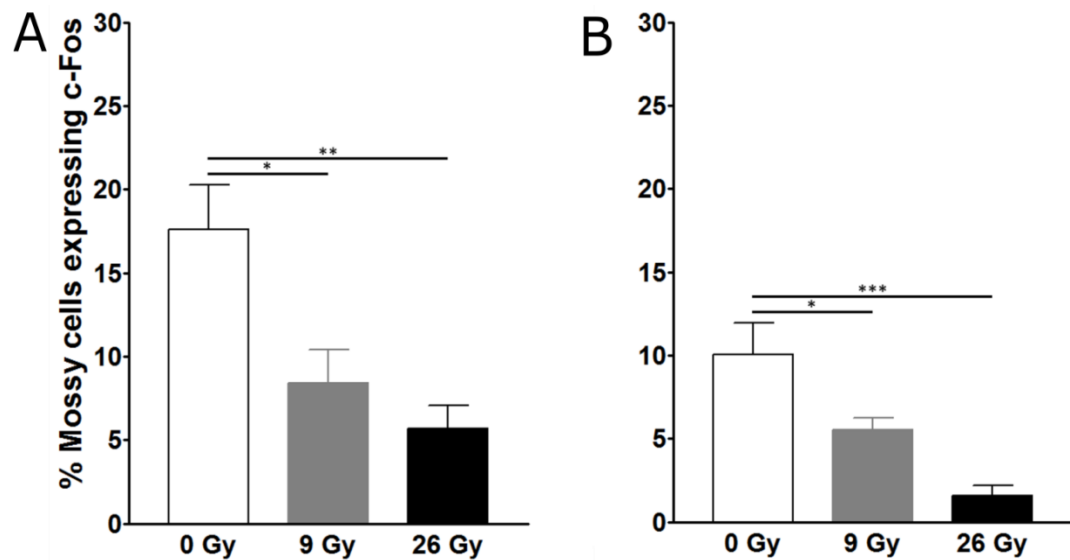


Figure 7. The proportion of mossy cells expressing *c-Fos* at 1-month (A) and 3 months (B) post radiotherapy. Data are expressed as mean \pm SEM. * $P < 0.05$, ** $P < 0.01$, *** $P < 0.001$; One-way ANOVA followed by Bonferroni's multiple comparisons post-hoc analysis.

Activity of Granule Cells

The activity of granule cells was measured through dual immunofluorescent staining for *c-Fos* and NeuN, a marker of mature neurons (EMD Millipore #ABN78). Four 20-30 z stack images (1 micron thick) were taken (two of each hippocampus per tissue) from two tissue sections of three different animals at each time point (72 at 1 month and 3 months post irradiation). Images were deconvoluted in AutoQuant X3 and analyzed in Imaris (BitPlane) to calculate the proportion of granule cells expressing *c-Fos* per image. Representative images can be seen in Figure 8.

One-Month Post Irradiation

Analysis yielded a significant difference between the group means at 1-month post irradiation (One-way ANOVA, $F=7.689$, $P=0.0019$; Figure 9A), with group averages of 1.1% at 0 Gy, 0.4% at 9 Gy, and 0.6% at 26 Gy. Bonferroni's multiple comparison test yielded a significant difference between 0 Gy and 9 Gy groups ($t=3.814$, $P<0.01$), 0 Gy and 26 Gy groups ($t=2.767$, $P<0.05$), but not between 9 Gy and 26 Gy groups ($t=1.071$, $P>0.05$). While the result between 0 Gy and 9 Gy groups was not significant, the group mean for 26 Gy was notably higher than 9 Gy.

Three Months Post Irradiation

Analysis at 3 months post irradiation resulted in a significant difference between the groups means (One-way ANOVA, $F=12.13$, $P<0.0001$; Figure 9B). The group means are 0.4% at 0 Gy, 0.1% at 9 Gy, and 0.3% at 26 Gy. When the group means were analyzed individually via Bonferroni's multiple comparison test, a significant difference was found between the group means of 0 Gy and 9 Gy ($t=4.817$, $P<0.001$), 9 Gy and 26 Gy ($t=3.297$, $P<0.01$), but not between 0 Gy and 26 Gy ($t=1.520$, $P>0.05$).

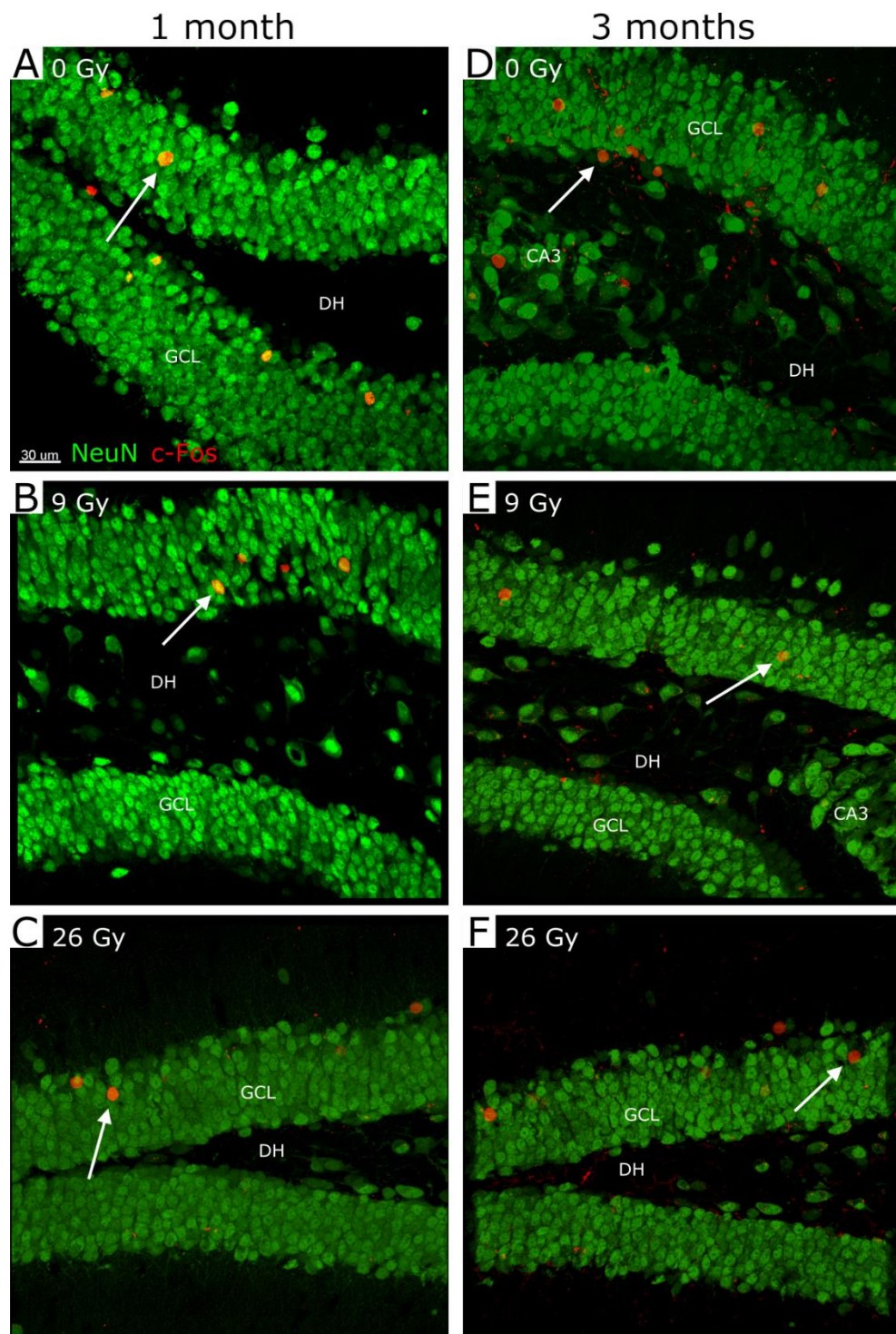


Figure 8. Immunofluorescent stains of granule cells expressing *c-Fos* at 1-month (A-C) and 3 months (D-F) post radiotherapy. Arrows indicate *c-Fos* labeling within the granule cell layer (GCL). DH dentate hilus.

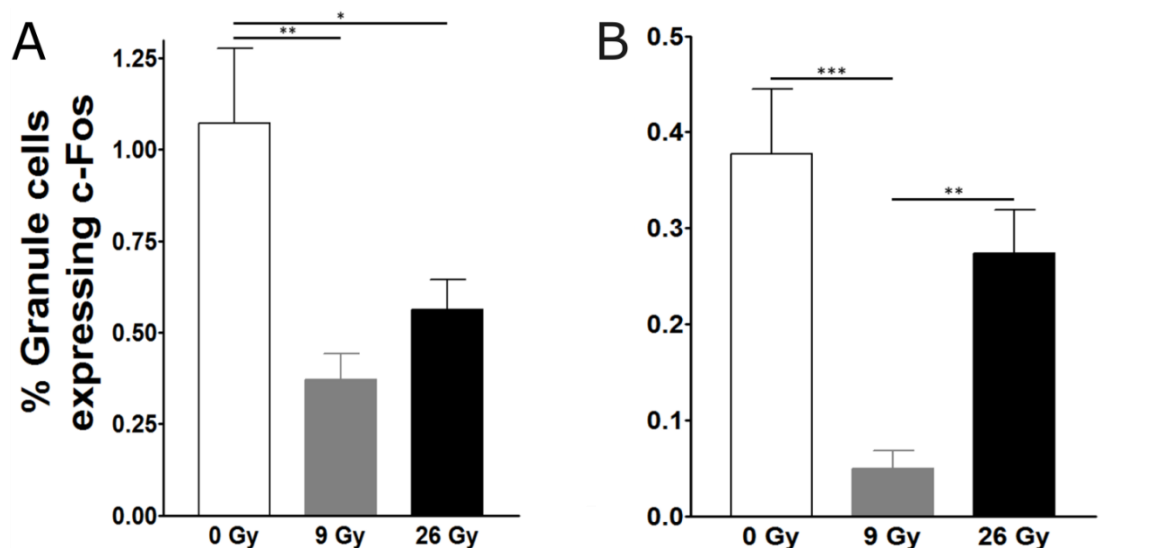


Figure 9. Quantification of the proportion of granule cells expressing *c-Fos* at 1 month (A) and 3 months (B) post radiotherapy. * $P < 0.05$, ** $P < 0.01$, *** $P < 0.001$.

Neurogenesis

Measurements of neurogenesis within the subgranular zone of the dentate gyrus were conducted via immunofluorescent staining of BrdU (EMD Millipore #MAB3424) and NeuN. Representative images can be seen in Figure 10.

One-Month Post Irradiation

A significant difference was found between the amount of dual labeled dentate granular cells between all group means (One-way ANOVA, $F=51.45$, $P < 0.0001$; Figure 11A), with a decrease of 83% and 97% at 9 Gy and 26 Gy, respectively. Bonferroni's multiple comparison test yielded a significant difference

between 0 Gy and 9 Gy groups ($t=8.131$, $P<0.001$), between 9 Gy and 26 Gy groups ($t=9.518$, $P<0.001$), but not between 9 Gy and 26 Gy groups ($t=1.455$, $P>0.05$).

Three months Post irradiation

A similar effect was seen at 3 months post irradiation, with a significant difference between group means (One-way ANOVA, $F=111.2$, $P<0.0001$; Figure 11B), with a decrease of 93% and 98% at 9 Gy and 26 Gy, respectively. When compared individually through Bonferroni's multiple comparison test, a significant difference was found between 0 Gy and 9 Gy groups ($t=12.54$, $P<0.001$), 0 Gy and 26 Gy groups ($t=13.26$, $P<0.001$), but not between 9 Gy and 26 Gy groups ($t=0.723$, $P>0.05$).

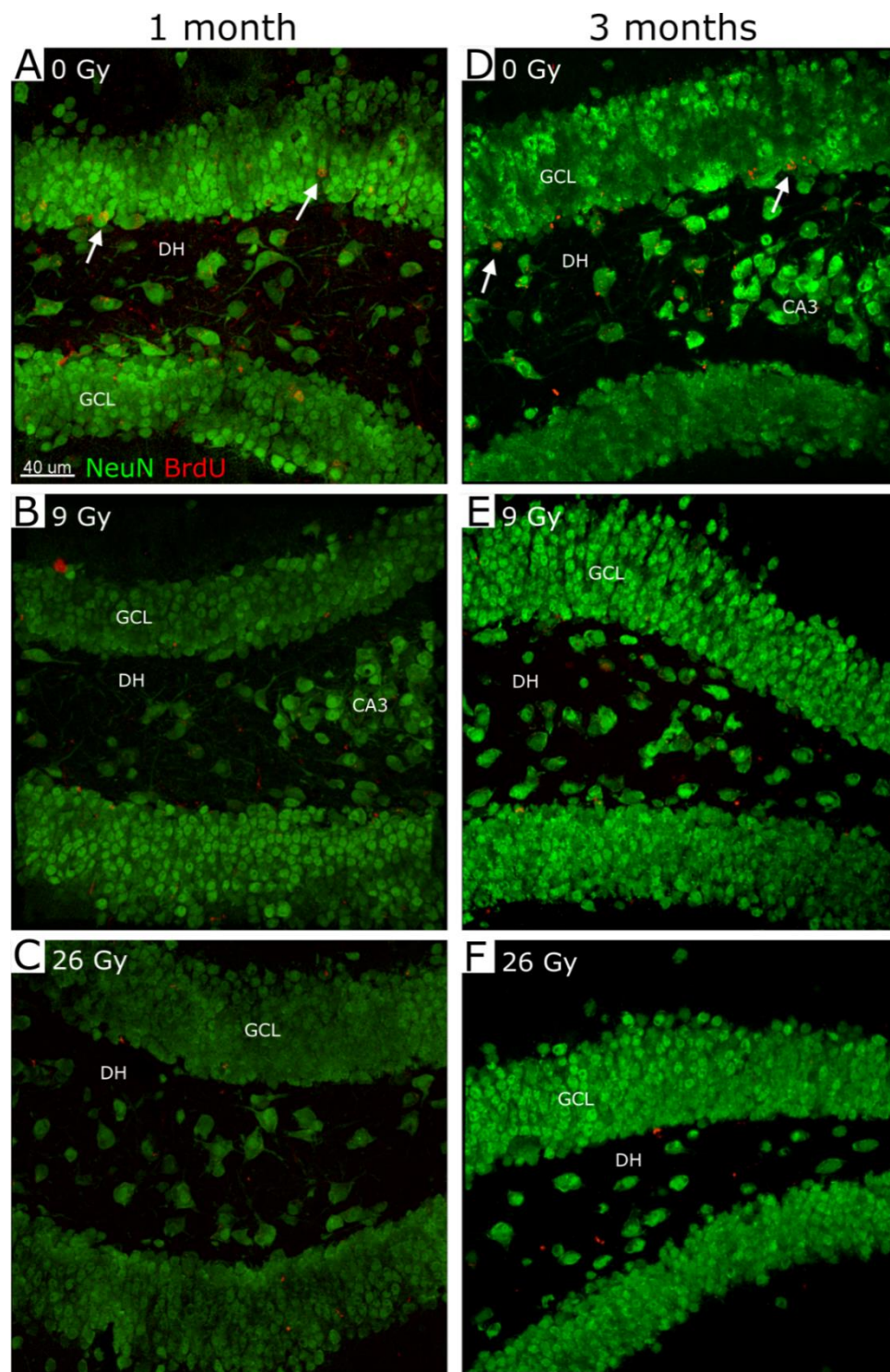


Figure 10. Immunofluorescent staining of granule cells labeled with BrdU at 1-month (A-C) and 3 months (D-F) post radiotherapy. Arrows indicate BrdU labeling in the granule cell layer (GCL). DH dentate hilus.

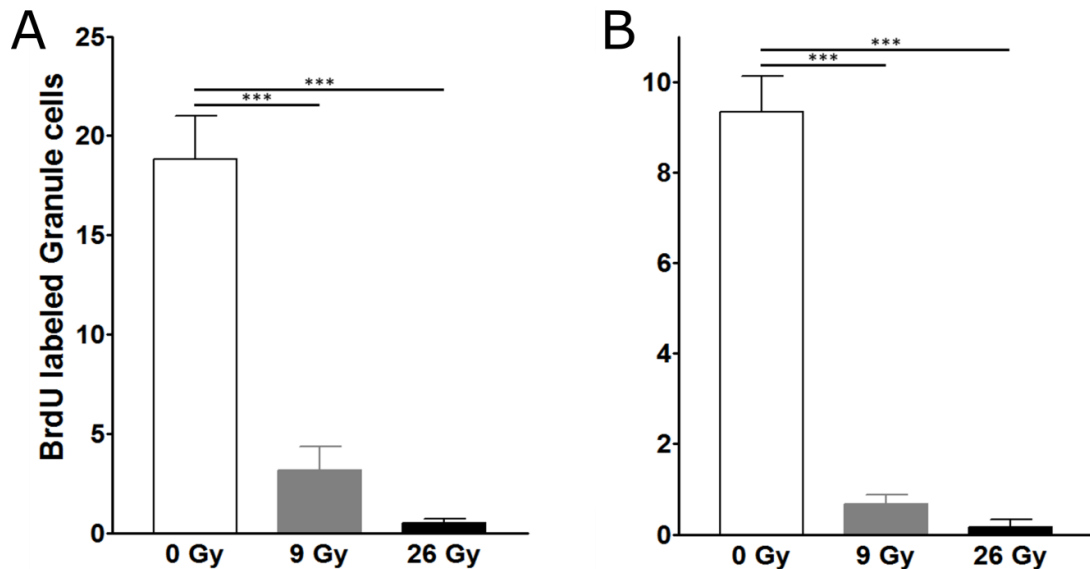


Figure 11. Quantification of the number of BrdU labeled granule cells at 1-month (A) and 3 months (B) post radiotherapy. Data are expressed as mean \pm SEM. *** $P < 0.001$; One-way ANOVA followed by Bonferroni's multiple comparisons post-hoc analysis.

C-Fos Induction in Response to Spatial Novelty

In order to quantify any difference in the spatially-induced *c-Fos*, its absolute levels within one hippocampus from each mouse were quantified via RT-qPCR 30 minutes after exposure to environmental novelty. Animals were tested and sacrificed 1-month post radiotherapy. Data are presented as the absolute ratio of *c-Fos* mRNA to Actin mRNA $\times 1000$. Cage control mice (four 0 Gy, four 9 Gy, and four 26 Gy mice not exposed to a novel environment) demonstrated no significant difference amongst group means (One-way ANOVA, $P = 0.2651$; Figure 12A). Exploration mice (four 0 Gy, four 9 Gy, and 4 26 Gy mice

exposed to environmental novelty) yielded a significant difference between group means (One-way ANOVA, $F=5.188$, $P=0.0359$; Figure 12B), with a significant difference found between the group means of 0 Gy and 26 Gy mice (Bonferroni's multiple comparisons test, $t=3.213$, $P<0.05$) but not between 0 Gy and 9 Gy ($t=1.864$, $P>0.05$) nor 9 Gy and 26 Gy ($t=1.291$, $P>0.05$).

Comparisons between respective irradiated groups (i.e. 0 Gy cage control mice vs. 0 Gy exploration mice) resulted in a significant difference 0 Gy mice (Student's unpaired t-test, two-tailed, $t=3.261$, $P=0.0224$; Figure 12C). No significant difference between group means was found for 9 Gy comparisons ($t=1.315$, $P=0.259$) and 26 Gy comparisons ($t=1.549$, $P=0.1821$; Figure 12C).

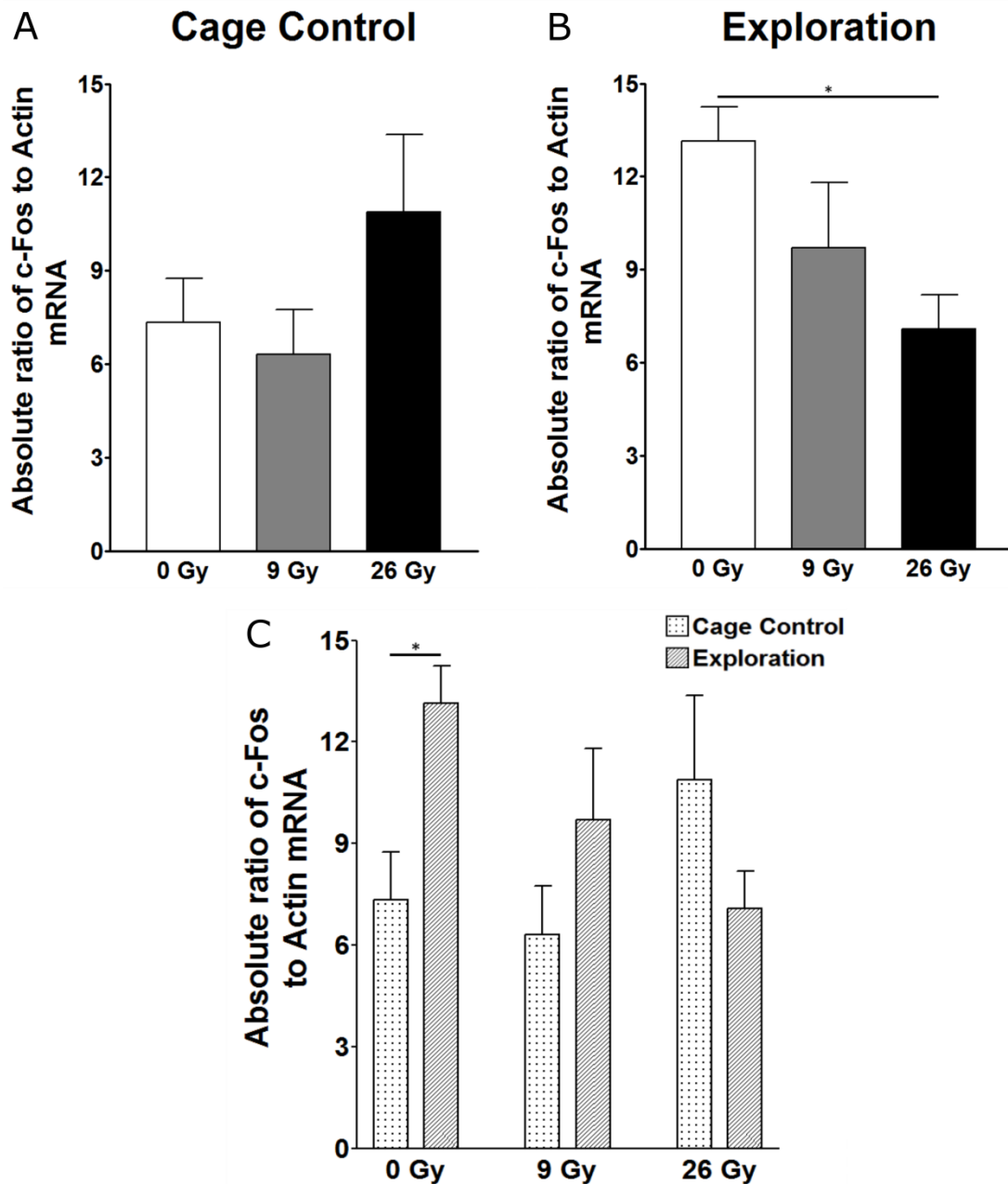


Figure 12. RT-qPCR results for *c-Fos* mRNA levels in the novel exploration experiment. Cage controls (A) showed no significant difference between the means of all groups. Exploration (B) demonstrated a significant difference between 0 Gy and 26 Gy. Comparisons between each radiation treatment (C) demonstrated only a significant difference between 0 Gy cage controls and 0 Gy exploration animals. * $P < 0.05$.

CHAPTER FIVE

DISCUSSION

Mossy Cell Loss Following Clinical Radiotherapy

The results here demonstrate that mossy cell numbers are reduced following clinically relevant doses of cranial x-ray irradiation. Mossy cells themselves are critical actors in understanding and memory of spatial context (Bui et al., 2018), and their loss here directly contributes to our understanding of how cranial radiotherapy can result in terminal cognitive decline, especially with respect to spatial navigation. Decrease of mossy cells between 1-month and 3-month control animals is an age-related effect. Interestingly, as there are latent progressive effects of ionizing radiation, there was no meaningful difference in the proportion of mossy cells lost when comparing 1-month (Figure 5D) and 3-month (Figure 5H) animals. Perhaps loss occurs immediately after treatment and does not progress further as time moves forward. This may to an extent be explained by functional differences amongst the mossy cell population. It is hypothesized that not all mossy cells within the dentate hilus share similar synaptic responses (Scharfman 2016) and that differences in activity of mossy cells occur in correlation with different regions of the dentate hilus (Scharfman 1991; Duffy et al., 2016; Bui et al., 2018). For example, many mossy cells express calretinin, a protein involved in calcium signaling, but only ventrally. (Fujise et al., 1997) Perhaps particular subsets of mossy cells with specific synaptic pathways correlate with different degrees of radioresistance.

The vulnerability of mossy cells is a currently an unexplained phenomenon, and several hypotheses for this exist (Scharfman, 2016), including low levels of autophagy (Yuan et al., 2015). Ionizing radiation causes radiolysis of water molecules, which causes oxidative stress to organelles, cellular molecules, and DNA. This damage elicits an autophagic response in cells. If mossy cells cannot handle the autophagic stress following radiotherapy, it may be the reason for the decline in numbers observed.

Mossy Cell Inactivity and Memory Impairment

The result found in this study suggest that basal activity levels of mossy cells are decreased under normal housing conditions following clinical radiotherapy. This decrease is still significant when corrected for total number of mossy cells per tissue. In addition, a decrease in activity is seen as one progresses from 1-month to 3 months in all group including controls (Fig 7A, B). This may be due to a total lack of novel stimulation within the housing cages.

While some mossy cells remain following radiotherapy, many of them are functionally impaired. Mossy cells are critical for trisynaptic circuitry within the hippocampus as well as providing net inhibitory signals to the dentate gyrus and considering an individual cell can innervate tens of thousands of other cells, the decrease in synaptic activity can have widespread implications.

The quantification of granule cells expressing *c-Fos* revealed a decrease in activity at 9 Gy and 26 Gy at 1 month, but not 26 Gy at 3 months. At 1-month post treatment, one can observe that the mean level of expression was higher at

26 Gy than 9 Gy (Fig 9A), and this trend continues into 3-months (Fig 9B). The ionizing radiation administered does not selectively target the mossy cells; it targets the brain as a whole, which means granule cells themselves are irradiated. Their loss of activity, or lack of, can be due to mixed effects from the dysfunction mossy cell and the radiation itself. Selective loss of mossy cells has been demonstrated to result in dentate granular hyperexcitability (Jinde et al., 2016, Bui et al., 2018). Mossy cells indirectly play major inhibitory role on granule cells, and if mossy cells are no longer providing the threshold of innervation to inhibitory interneurons (as is the case with epileptic seizures), or the interneurons are dysfunctional themselves, granule cells may become hyperexcitable. Further study is needed to understand granule cell responses to ionizing radiation.

Mossy Cells and Neurogenesis

The results observed in this study (Figure 11A, 11B) contribute to the body of evidence suggesting radiation depletes neurogenesis within the hippocampus. The loss of mossy cells seen here correlates with the impaired hippocampal neurogenesis. While radiation is known to deplete proliferating cells, it may not be entirely responsible for their inability to recover from this trauma. Very few granule cells are labeled with BrdU in both irradiated groups (9 Gy and 26 Gy, Figure 10B, 10C 10E, and 10F) even three months post cranial radiotherapy. With consideration of how mossy cells have a critical role as a major niche in integration and maturation of adult-born granule cells, there is reason to suspect that both the loss of these cells and loss of their activity may contribute to the

lack of reinstatement of neurogenesis within the subgranular zone. If postnatally born neurons never reach maturity, are unable to integrate into existing tissue and die off due to lack of functional synaptic input, then neurogenesis is incomplete and ineffective. With consideration to mossy cell knockout models and impaired pattern separation (Jinde et al., 2012), any loss of mossy cells due to ionizing radiation can result in similar effects. I hypothesize that without properly functioning mossy cells, neurogenesis at least partially is substantially inhibited in the cranial irradiated brain.

Epigenetic Regulation of *c-Fos*

No significant difference was observed between cage control animals (Figure 12A), suggesting all baseline mRNA levels were similar. However, while not significant, 26 Gy cage control mice demonstrated elevated *c-Fos* mRNA levels, which correlates with the increase in *c-Fos* expression observed in granule cells. This may be due to decreased numbers and activity of mossy cells.

Animals exposed to environmental novelty was sufficient to induce the expression of *c-Fos*, as transcript levels were higher in the exploratory 0 Gy group compared to the cage control 0 Gy group (Figure 12C). Further, no significant difference was found between cage control and exploration animal mRNA levels for neither 9 Gy nor 26 Gy (Figure 12C). Head-only ionizing radiation was sufficient to inhibit the transcription of this gene. This result suggests that clinically relevant doses of radiotherapy can diminish transcript levels of *c-Fos* induced by functional behavior paradigms. In addition, a visible

trend is present in the transcript levels for exploration animals (Figure 12B), indicating that the extent of the induction may be dose-dependent.

The expression of IEGs and *c-Fos* are dependent on specific external stimuli. If the production of transcripts is inhibited, it may be due to methylation of the gene of interest. Based on the result seen here, the *c-Fos* gene may be a target of radiation-induced epigenetic modulation. To determine if this is the case, a closer look at the methylation status of the gene and its promoter is recommended.

With both a decrease in the number of mossy cells and decreases in cellular activity, this thesis supports the hypothesis that mossy cells can contribute to the mechanisms associated with radiation-induced cognitive decline. Restoring mossy cell function can be a potential target for treating this condition. In addition to adding ionizing radiation to the list of neurotoxic insults, this study demonstrates *in vivo* the hippocampus has reduced sensitivity to spatial novelty.

APPENDIX A
ANTIBODIES

Table 2. Information about antibodies used for immunohistochemistry.

Antibody	Supplier	Catalog #	Concentration	Marker for:
Rabbit anti GluR2/3	EMD Millipore	AB1506	Bright field: 1:100 Confocal: 1:400	Mossy cells
Mouse anti <i>c-Fos</i> [2H2]	Abcam	ab208942	Confocal: 1:1000	Activity/Novelty/Memory
Mouse anti Prox1	Novus Biologicals	5G10	Confocal: 1:250	Ectopic granule cells
Mouse anti BrdU	EMD Millipore	MAB3424	Confocal: 1:400	Proliferation, Adult-born granule cells
Rabbit anti NeuN	EMD Millipore	ABN78	Confocal: 1:400	Mature neurons
Biotinylated Goat anti Rabbit IgG	Vector Labs	AB-1000	Bright field: 1:400	Bright field secondary antibody
Donkey anti Mouse IgG AF 594	Thermo Scientific	A-21203	Confocal: 1:800	Immunofluorescent secondary antibody
Donkey anti Rabbit IgG AF 488	Thermo Scientific	A-21206	Confocal: 1:800	Immunofluorescent secondary antibody
Donkey anti Mouse IgG AF 488	Thermo Scientific	A-21202	Confocal: 1:800	Immunofluorescent secondary antibody
Donkey anti Rabbit IgG AF 594	Thermo Scientific	A-21207	Confocal: 1:800	Immunofluorescent secondary antibody
4',6-diamidino-2- phenylindole (DAPI)	Thermo- Scientific	62248	1 mg/ml	Nucleus

APPENDIX B

IMMUNOHISTOCHEMICAL PROTOCOLS

GluR2/3 *c-Fos* Immunofluorescence Stain

Day 1

1. Collect tissues in 24 well plates. 3 tissues max per well
2. Wash three times with PBS -/- 5 minutes each
3. **Blocking:** 10% Normal Donkey Serum (NDS), 0.01% Triton-X 100, PBS -/- for 30 minutes
4. **Primary Antibody:** 2% NDS, 0.01% TRITON-X 100, Rabbit anti GluR2/3 (EMD Millipore #1506) (1:250), Mouse anti *c-Fos* [2H2] (Abcam ab208942) (1:1000) PBS -/- overnight at 4C.

Day 2

5. Keep tissues on shaker for 1 hour.
6. Wash tissues 3 times with PBS 5 minutes each.
7. **Secondary Antibody:** Donkey anti Mouse AF488 (1:800), Donkey anti Rabbit AF594 (1:800), 2% NDS, 0.01% TRITON-X 100, PBS.

1mL = 2.5 uL Donkey anti mouse AF488, 2.5 uL Donkey anti rabbit AF594, 100 uL NDS, 100 uL 10% TRITON-X 100.

For 1 hour in the dark

8. Wash three times PBS 5 minutes each.
9. **DAPI:** 0.5X DAPI in PBS for 5-7 minutes.
10. Wash three times with PBS 5 minutes each.
11. Mount tissue sections using SlowFade gold.

NeuN + *c-Fos* Immunostaining

Day 1

1. Pick up sections in 24-well plate. 3 sections per well max.
2. Wash tissues 3 times in PBS, 5 minutes each.
3. **Blocking:** 10% Normal Donkey Serum (NDS) + 0.1% TRITON-X 100 + PBS. Incubate sections for 30 minutes.
 - a. 1 mL = 100 uL NDS + 100 uL of 10% TRITON-X 100-100 + PBS
4. **Primary Antibody:** 10% NDS + 0.1% TRITON-X 100 + Rabbit anti NeuN (1:400) + Mouse anti *c-Fos* (1:1000).
 - a. 100 uL NDS
+ 100 uL of 10% TRITON-X 100-100
+ 2.5 uL Rb anti NeuN
+ 1.0 uL M anti *c-Fos*
+ PBS to 1 mL
Incubate sections overnight in 4C refrigerator.

Day 2

5. Place sections on a shaker for 1 hour.
6. Wash sections 3 times in PBS 5 minutes each.
7. **Secondary Antibody:** 10% NDS + 0.1% TRITON-X 100 + Donkey anti Rabbit AF 488 (1:400)
 - a. 100 uL NDS
+ 100 uL 10% TRITON-X 100-
+ 2.5 uL Dk anti Rb AF488
+ 2.5 uL Dk anti M AF594
+ PBS to 1 mL
Incubate sections for 1 hour in the dark.
8. Wash sections 3 times in PBS 5 minutes each.
9. Incubate sections in 0.5X DAPI for 5-7 minutes.
10. Wash sections 3 times in PBS 5 minutes each.
11. Mount sections on microscope slides using SlowFade mounting media.

BrdU Immunofluorescence for double immuno-staining

Day 1

1. Pick up sections in PBS one day prior to staining (to remove residual Freezing solution)
2. Washing: 2x PBS
5' ea
3. 10% Methanol (ice cold) – keep plates on ice
20 min
(10 ml: 9 ml PBS + 1 ml 100% MeOH, keep on ice)
3. Washing: 3x PBS
5' ea
4. **Formamide Treatment:**
Incubate in 50% formamide solution, 50% 2x SSC buffer (Sigma)
65-69°C 2hr
[2X SSC buffer: 2ml 20X SSC + 8 ml MQ water] – store at 4C, refrigerator
4. Washing 3x in Cold SSC buffer
5' ea
5. **2N HCl treatment** (5 ml Conc. HCl + 10 ml PBS + 10 ml D/w)
30' at 37°C
6. **Borate treatment:** 0.1 M Borate buffer (**pH 8.5**)
10' at RT
7. Washing: 2x PBS
5' ea
8. **Blocking:** 10% NDS + 0.1% TX-100
30' RT
(10 ml PBS + 1 ml NDS + 25 µl TX-100)
9. **Primary Antibody:** Mouse anti-BrdU (1:400) **Millipore MAB3424** + Rb anti-NeuN (1:500)

Day 2

10. Washing: 3x PBS
5' ea
11. **Secondary Antibody:** [Donkey-Anti-Mouse AF 594, **1:200**] + [Donkey-anti-Rabbit AF 488, 1:500]
1h, RT
12. Wash with Distilled water (don't exceed more than 2min)
2' ea
13. Washing: 3x PBS
5' ea
14. Mount sections using SlowFade Antifade
15. Observe under fluorescence microscope: BrdU (Red) and NeuN (Green)

Mossy Cell (GluR2/3 Millipore AB#1506) Bright field Staining

Protocol is adapted and modified from Duffy et al., 2013

Day 1

All steps done on a shaker at low setting

1. Wash sections in 0.1M TBS 3 times 5 minutes each.
2. Incubate in 1% hydrogen peroxide in 0.1M TBS for 2 minutes.
3. Wash sections 3 times 5 minutes each in 0.1M TBS
4. Incubate in TBS-A (0.1% TRITON-X 100 in 0.1M Tris buffer) 10 minutes
5. Incubate in TBS-B (0.1% TRITON-X 100 and 0.005% bovine serum albumin (BSA) in 0.1M TBS) 10 minutes. 4% BSA to 0.005% BSA = 125 μ L of 4% BSA in TBS
6. Block (10% NGS in 0.1M Tris, 0.25% TRITON-X 100, 0.005% BSA) for 1 hour
 - a. 0.005% BSA from 4% BSA = 125 μ L of 4% BSA per 1 mL of TBS
7. Wash in Tris A 10 minutes
8. Wash in Tris B 10 minutes
9. **Incubate in primary antibody** (Rabbit anti GluR2/3 1:100) **for 24 hours on shaker at room temp.**
 - a. 10% NGS in TBS-A

Day 2

10. 23 hours in, keep tissue on shaker for 1 hour.
11. Wash 10 minutes in TBS-A
12. Wash 10 minutes TBS-B
13. **Incubate with secondary antibody** (goat anti-rabbit 1:400 vector labs #AB-1000) **for 1 hour** in TBS-A.
 - a. 1:400 Gt anti Rb biotin, 2% NGS, 0.1% TRITON-X 100 in TBS.
14. Wash with TBS-A 10 minutes
15. Wash in TBS-B 10 minutes
16. **Incubate in ABC complex for 2 hours.** Vectorlabs ABC HRP Elite #PK-1000 ABC kit: 2 drops A, 2 drops B, in 4mL prepared 30 minutes before incubation. In Tris-D (0.5M Tris B)
17. Wash in 0.1M Tris 3x 5 minutes
18. Incubate sections using a DAB kit.
 - a. 2mL distilled water 2mL TBS
 - b. 2 drops of buffer stock solution (~84 μ L)
 - c. 2 drops of DAB stock solution (~50 μ L)
 - d. 2 drops of Hydrogen Peroxide Solution (~80 μ L)
 - e. 2 drops of nickel solution (~80 μ L)
 - f. Mix and incubate for 2-10 minutes. Depends on intensity of color development.
 - g. GluR2/3 – 5 minutes per section.

19. Wash sections 3x 5minutes each in Tris 0.1M.
20. Mount sections and dry overnight
21. Alcohol series hydration
 - a. 100% ethanol 5 minutes, 95% ethanol 3 minutes, 70% ethanol 3 minutes, 50% ethanol 3 minutes, distilled water 3 minutes
22. Counterstain with nuclear fast red for 2 minutes
23. Alcohol series dehydration
 - a. 1% HCl 3 dips, tap water 10 minutes, distilled water 3 minutes, 50% ethanol 3 minutes, 70% ethanol 3 minutes, 95% ethanol 3 minutes, 100% ethanol 5 minutes twice, xylenes 5 minutes twice.
24. Coverslip with 50% xylene, 50% Permount mounting media.

GluR2/3 + Prox1 Immunofluorescence Stain

Day 1

1. Collect tissues in 24 well plates. 3 tissues max per well
2. Wash three times with PBS -/- 5 minutes each
3. **Blocking:** 10% Normal Donkey Serum, 0.01% TRITON-X 100, PBS -/- for 30 minutes
4. **Primary Antibody:** 2% NDS, 0.01% TRITON-X 100, Rabbit anti GluR2/3 (EMD Millipore #1506) (1:400), Mouse anti Prox1 (Novus Biologicals 5G10) (1:250) PBS -/- overnight at 4C. (100 uL of 10% TRITON-X 100)

Day 2

5. Keep tissues on shaker for 1 hour.
6. Wash tissues 3 times with PBS 5 minutes each.
7. **Secondary Antibody:** Donkey anti Mouse AF488 (1:800), Donkey anti Rabbit AF594 (1:800), 2% NDS, 0.01% TRITON-X 100, PBS.

1mL = 2.5 uL Donkey anti mouse AF488, 2.5 uL Donkey anti rabbit AF594, 100 uL NDS, 100 uL 10% TRITON-X 100.

For 1 hour in the dark

8. Wash three times PBS 5 minutes each.
9. **DAPI:** 0.5X DAPI in PBS for 5-7 minutes.
10. Wash three times with PBS 5 minutes each.
11. Mount tissue sections using SlowFade gold.

REFERENCES

- Abta.org. (2017). *Brain Tumor Statistics | American Brain Tumor Association*.
[online] Available at: <http://www.abta.org/about-us/news/brain-tumor-statistics/> [Accessed 10 Nov. 2017].
- Acharya, M., Baddour, A., Kawashita, T., Allen, B., Syage, A., Nguyen, T., Yoon, N., Giedzinski, E., Yu, L., Parihar, V. and Baul Acharya, M., Baddour, A., Kawashita, T., Allen, B., Syage, A., Nguyen, T., Yoon, N., Giedzinski, E., Yu, L., Parihar, V. and Baulch, J. (2017). Epigenetic determinants of space radiation-induced cognitive dysfunction. *Scientific Reports*, 7, p.42885.
- Acharya, M., Christie, L., Lan, M., Donovan, P., Cotman, C., Fike, J., Limoli, C. (2009). Rescue of radiation-induced cognitive impairment through cranial transplantation of human embryonic stem cells. *Proceedings of the National Academy of Sciences*, 106(45), pp.19150-19155.
- Acharya, M., Christie, L., Lan, M., Giedzinski, E., Fike, J., Rosi, S. and Limoli, C. (2011). Human neural stem cell transplantation ameliorates radiation-induced cognitive dysfunction. *Cancer Research*, 71(14), pp.4834-4845.
- Acharya, M., Patel, N., Craver, B., Tran, K., Giedzinski, E., Tseng, B., Parihar, V., Limoli, C. (2015). Consequences of low dose ionizing radiation exposure on the hippocampal microenvironment. *PLoS One*, 10(6), p.e0128316.

- Agostinho, P., A. Cunha, R. and Oliveira, C. (2010). Neuroinflammation, oxidative stress and the pathogenesis of alzheimers disease. *Current Pharmaceutical Design*, 16(25), pp.2766-2778.
- Antwih, D., Gabbara, K., Lancaster, W., Ruden, D., & Zielske, S. (2013). Radiation-induced epigenetic DNA methylation modification of radiation-response pathways. *Epigenetics*, 8(8), 839-848.
<http://dx.doi.org/10.4161/epi.25498>
- Baldwin, S., Gibson, T., Callihan, C., Sullivan, P., Palmer, E. and Scheff, S. (1997). Neuronal cell loss in the CA3 subfield of the hippocampus following cortical contusion utilizing the optical disector method for cell counting. *Journal of Neurotrauma*, 14(6), pp.385-398.
- Baulch, J. E., Acharya, M. M., Allen, B. D., Ru, N., Chmielewski, N. N., Martirosian, V., ... Limoli, C. L. (2016). Cranial grafting of stem cell-derived microvesicles improves cognition and reduces neuropathology in the irradiated brain. *Proceedings of the National Academy of Sciences of the United States of America*, 113(17), 4836–4841.
<http://doi.org/10.1073/pnas.1521668113>
- Bertaina-Anglade, V., Tramu, G. and Destrade, C. (2000). Differential learning-stage dependent patterns of *c-Fos* protein expression in brain regions during the acquisition and memory consolidation of an operant task in mice. *European Journal of Neuroscience*, 12(10), pp.3803-3812.

- Bird, C. and Burgess, N. (2008). The hippocampus and memory: insights from spatial processing. *Nature Reviews Neuroscience*, 9(3), pp.182-194.
- Brown, P., Pugh, S., Laack, N., Wefel, J., Khuntia, D., Meyers, C., Choucair, A., Fox, S., Suh, J., Roberge, D., Kavadi, V., Bentzen, S., Mehta, M. and Watkins-Bruner, D. (2013). Memantine for the prevention of cognitive dysfunction in patients receiving whole-brain radiotherapy: a randomized, double-blind, placebo-controlled trial. *Neuro-Oncology*, 15(10), pp.1429-1437.
- Buckmaster, P., Wenzel, H., Kunkel, D. and Schwartzkroin, P. (1996). Axon arbors and synaptic connections of hippocampal mossy cells in the rat in vivo. *The Journal of Comparative Neurology*, 366(2), pp.270-292.
- Bui, A., Nguyen, T., Limouse, C., Kim, H., Szabo, G., & Felong, S. et al. (2018). Dentate gyrus mossy cells control spontaneous convulsive seizures and spatial memory. *Science*, 359(6377), 787-790.
<http://dx.doi.org/10.1126/science.aan4074>
- Cameron, H. and McKay, R. (2001). Adult neurogenesis produces a large pool of new granule cells in the dentate gyrus. *The Journal of Comparative Neurology*, 435(4), pp.406-417.
- Cancer.Gov. (2017). *Radiation Therapy for Cancer | National Cancer Institute*.
[online] Available at: <https://www.cancer.gov/about->

cancer/treatment/types/radiation-therapy/radiation-fact-sheet National Cancer Institute [Accessed 10 Nov. 2017].

Cancer.Net. (2017). *Brain Tumor | American Society of Clinical Oncology*.

[online] Available at: <http://www.cancer.net/cancer-types/brain-tumor/symptoms-and-signs>. American Society of Clinical Oncology [Accessed 10 Nov. 2017].

Chancey, J., Poulsen, D., Wadiche, J. and Overstreet-Wadiche, L. (2014). Hilar mossy cells provide the first glutamatergic synapses to adult-born dentate granule cells. *Journal of Neuroscience*, 34(6), pp.2349-2354.

Cheah, S., Lawford, B., Young, R., Morris, C. and Voisey, J. (2015). Dysbindin (DTNBP1) variants are associated with hallucinations in schizophrenia. *European Psychiatry*, 30(4), pp.486-491.

Clelland, C., Choi, M., Romberg, C., Clemenson, G., Fragniere, A., Tyers, P., Jessberger, S., Saksida, L., Barker, R., Gage, F. and Bussey, T. (2009). A functional role for adult hippocampal neurogenesis in spatial pattern separation. *Science*, 325(5937), pp.210-213.

Danielson, N., Turi, G., Ladow, M., Chavlis, S., Petrantonakis, P., Poirazi, P. and Losonczy, A. (2017). In vivo imaging of dentate gyrus mossy cells in behaving mice. *Neuron*, 93(3), pp.552-559.e4.

- Deng, W., Saxe, M., Gallina, I. and Gage, F. (2009). Adult-born hippocampal dentate granule cells undergoing maturation modulate learning and memory in the brain. *Journal of Neuroscience*, 29(43), pp.13532-13542.
- Douw, L., Klein, M., Fagel, S., van den Heuvel, J., Taphoorn, M., Aaronson, N., Postma, T., Vandertop, W., Mooij, J., Boerman, R., Beute, G., Sluimer, J., Slotman, B., Reijneveld, J. and Heimans, J. (2009). Cognitive and radiological effects of radiotherapy in patients with low-grade glioma: long-term follow-up. *The Lancet Neurology*, 8(9), pp.810-818.
- Duffy, A., Schaner, M., Chin, J. and Scharfman, H. (2013). Expression of *c-Fos* in hilar mossy cells of the dentate gyrus in vivo. *Hippocampus*, 23(8), pp.649-655.
- Edelstein, K., Spiegler, B., Fung, S., Panzarella, T., Mabbott, D., Jewitt, N., D'Agostino, N., Mason, W., Bouffet, E., Tabori, U., Laperriere, N. and Hodgson, D. (2011). Early aging in adult survivors of childhood medulloblastoma: long-term neurocognitive, functional, and physical outcomes. *Neuro-Oncology*, 13(5), pp.536-545.
- Falkai, P. and Bogerts, B. (1986). Cell loss in the hippocampus of schizophrenics. *European Archives of Psychiatry and Neurological Sciences*, 236(3), pp.154-161.
- Fujise, N., Liu, Y., Hori, N., & Kosaka, T. (1997). Distribution of calretinin immunoreactivity in the mouse dentate gyrus: II. Mossy cells, with special

- reference to their dorsoventral difference in calretinin immunoreactivity. *Neuroscience*, 82(1), 181-200.
- Garden, G. (2013). Epigenetics and the modulation of neuroinflammation. *Neurotherapeutics*, 10(4), pp.782-788.
- Gray, H. (1918). *Anatomy of the Human Body*. Philadelphia, PA: Lea & Febiger.
- Guzowski, J.F., McNaughton, B.L., Barnes, C.A., and Worley, P.F. (1999). Environment-specific expression of the immediate-early gene Arc in hippocampal neuronal ensembles. *Nature Neuroscience*, 2(12), pp.1120-4.
- Hall, E. J., Giaccia, A. J. (2006) *Radiobiology for the radiologist*. Philadelphia, PA: Lippincott Williams & Wilkins.
- Henze, D., Urban, N. and Barrionuevo, G. (2000). The multifarious hippocampal mossy fiber pathway: a review. *Neuroscience*, 98(3), pp.407-427.
- Hitti, F. and Siegelbaum, S. (2014). The hippocampal CA2 region is essential for social memory. *Nature*, 508(7494), pp.88-92.
- Hsu, M., Buzsaki, G. (1993). Vulnerability of mossy fiber targets in the rat hippocampus to forebrain ischemia. *The Journal of Neuroscience*, 13(9), pp.3964-3979.

- Huang, T., Zou, Y. and Corniola, R. (2012). Oxidative stress and adult neurogenesis—effects of radiation and superoxide dismutase deficiency. *Seminars in Cell & Developmental Biology*, 23(7), pp.738-744.
- Ji, J. and Maren, S. (2008). Differential roles for hippocampal areas CA1 and CA3 in the contextual encoding and retrieval of extinguished fear. *Learning & Memory*, 15(4), pp.244-251.
- Jinde, S., Zsiros, V., Jiang, Z., Nakao, K., Pickel, J., Kohno, K., Belforte, J., Nakazawa, K. (2012). Hilar mossy cell degeneration causes transient dentate granule cell hyperexcitability and impaired pattern separation. *Neuron*, 76(6), pp.1189-1200.
- Kohman, R., Bhattacharya, T., Wojcik, E. and Rhodes, J. (2013). Exercise reduces activation of microglia isolated from hippocampus and brain of aged mice. *Journal of Neuroinflammation*, 10(1).
- Magloczky, Z. and Freund, T. (1993). Selective neuronal death in the contralateral hippocampus following unilateral kainate injections into the CA3 subfield. *Neuroscience*, 56(2), pp.317-335.
- Martin-Fardon, R., Ciccocioppo, R., Aujla, H. and Weiss, F. (2007). The dorsal subiculum mediates the acquisition of conditioned reinstatement of cocaine-seeking. *Neuropsychopharmacology*, 33(8), pp.1827-1834.
- McGinty, J., Henriksen, S., Goldstein, A., Terenius, L. and Bloom, F. (1983). Dynorphin is contained within hippocampal mossy fibers: immunochemical

alterations after kainic acid administration and colchicine-induced neurotoxicity. *Proceedings of the National Academy of Sciences*, 80(2), pp.589-593.

Nakashiba, T., Cushman, J., Pelkey, K., Renaudineau, S., Buhl, D., McHugh, T., Barrera, V., Chittajallu, R., Iwamoto, K., McBain, C., Fanselow, M. and Tonegawa, S. (2012). Young dentate granule cells mediate pattern separation, whereas old granule cells facilitate pattern completion. *Cell*, 149(1), pp.188-201.

Nokia, M., Lensu, S., Ahtiainen, J., Johansson, P., Koch, L., Britton, S. and Kainulainen, H. (2016). Physical exercise increases adult hippocampal neurogenesis in male rats provided it is aerobic and sustained. *The Journal of Physiology*, 594(7), pp.1855-1873.

Owen, M., Williams, N. and O'Donovan, M. (2004). Dysbindin-1 and schizophrenia: from genetics to neuropathology. *Journal of Clinical Investigation*, 113(9), pp.1255-1257.

Parihar, V. and Limoli, C. (2013). Cranial irradiation compromises neuronal architecture in the hippocampus. *Proceedings of the National Academy of Sciences*, 110(31), pp.12822-12827.

Parihar, V., Pasha, J., Tran, K., Craver, B., Acharya, M. and Limoli, C. (2014). Persistent changes in neuronal structure and synaptic plasticity caused by proton irradiation. *Brain Structure and Function*, 220(2), pp.1161-1171.

- Ramón y Cajal, S. (1911). *Histologie du système nerveux de l'homme et des vertébrés*. Paris, France: Maloine.
- Reimers, T., Ehrenfels, S., Mortensen, E., Schmiegelow, M., Sønderkaer, S., Carstensen, H., Schmiegelow, K. and Müller, J. (2002). Cognitive deficits in long-term survivors of childhood brain tumors: identification of predictive factors. *Medical and Pediatric Oncology*, 40(1), pp.26-34.
- Rola, R., Fishman, K., Baure, J., Rosi, S., Lamborn, K., Obenaus, A., Nelson, G. and Fike, J. (2008). Hippocampal neurogenesis and neuroinflammation after cranial irradiation with ⁵⁶Fe particles. *Radiation Research*, 169(6), pp.626-632.
- Rola, R., Raber, J., Rizk, A., Otsuka, S., VandenBerg, S., Morhardt, D. and Fike, J. (2004). Radiation-induced impairment of hippocampal neurogenesis is associated with cognitive deficits in young mice. *Experimental Neurology*, 188(2), pp.316-330.
- Rosi, S., Andres-Mach, M., Fishman, K., Levy, W., Ferguson, R. and Fike, J. (2008). Cranial irradiation alters the behaviorally induced immediate-early gene arc (activity-regulated cytoskeleton-associated protein). *Cancer Research*, 68(23), pp.9763-9770.
- Scharfman, H. (1994). Synchronization of area CA3 hippocampal pyramidal cells and non-granule cells of the dentate gyrus in bicuculline-treated rat hippocampal slices. *Neuroscience*, 59(2), pp.245-257.

- Scharfman, H. (2016). The enigmatic mossy cell of the dentate gyrus. *Nature Reviews Neuroscience*, 17(9), pp.562-575.
- Scharfman, H., Goodman, J. and McCloskey, D. (2006). Ectopic granule cells of the rat dentate gyrus. *Developmental Neuroscience*, 29(1-2), pp.14-27.
- Seress, L. and Ribak, C. (1995). Postnatal development of CA3 pyramidal neurons and their afferents in the Ammon's horn of rhesus monkeys. *Hippocampus*, 5(3), pp.217-231.
- Seress, L., Ábrahám, H., Horváth, Z., Dóczi, T., Janszky, J., Klemm, J., Byrne, R. and Bakay, R. (2009). Survival of mossy cells of the hippocampal dentate gyrus in humans with mesial temporal lobe epilepsy. *Journal of Neurosurgery*, 111(6), pp.1237-1247.
- Shaw, E., Rosdhal, R., D'Agostino, R., Lovato, J., Naughton, M., Robbins, M. and Rapp, S. (2006). Phase II study of donepezil in irradiated brain tumor patients: effect on cognitive function, mood, and quality of life. *Journal of Clinical Oncology*, 24(9), pp.1415-1420.
- Snyder, J., Choe, J., Clifford, M., Jeurling, S., Hurley, P., Brown, A., Kamhi, J. and Cameron, H. (2009). Adult-born hippocampal neurons are more numerous, faster maturing, and more involved in behavior in rats than in mice. *Journal of Neuroscience*, 29(46), pp.14484-14495.

- Tauck, D.L., Nadler, J.V. (1985). Evidence of functional mossy fiber sprouting in hippocampal formation of kainic acid-treated rats. *Journal of Neuroscience*, 5(4), pp.1016-22.
- Vago, D. and Kesner, R. (2008). Disruption of the direct perforant path input to the CA1 subregion of the dorsal hippocampus interferes with spatial working memory and novelty detection. *Behavioural Brain Research*, 189(2), pp.273-283.
- VanElzakker, M., Fevurly, R., Breindel, T. and Spencer, R. (2008). Environmental novelty is associated with a selective increase in Fos expression in the output elements of the hippocampal formation and the perirhinal cortex. *Learning & Memory*, 15(12), pp.899-908.
- Wang, H., Yuan, Y., Zhang, Z., Yan, H., Feng, Y. and Li, W. (2014). Dysbindin-1C is required for the survival of hilar mossy cells and the maturation of adult newborn neurons in dentate gyrus. *Journal of Biological Chemistry*, 289(42), pp.29060-29072.
- Wang, J., Zhang, Y., Xu, K., Mao, X., Xue, L., Liu, X., Yu, H., Chen, L. and Chu, X. (2014). Genome-wide screen of DNA methylation changes induced by low dose x-ray radiation in mice. *PLoS One*, 9(3), p.e90804.
- Yuan, Y., Wang, H., Wei, Z. and Li, W. (2015). Impaired autophagy in hilar mossy cells of the dentate gyrus and its implication in schizophrenia. *Journal of Genetics and Genomics*, 42(1), pp.1-8.

- Zhang, L., Sun, R. and Tian, Y. (2011). Dose-response relationship for radiation-induced cognitive impairment. *International Journal of Radiation Oncology, Biology, Physics*, 81(2), p.S727.
- Zhou, K., Boström, M., Ek, C., Li, T., Xie, C., Xu, Y., Sun, Y., Blomgren, K. and Zhu, C. (2017). Radiation induces progenitor cell death, microglia activation, and blood-brain barrier damage in the juvenile rat cerebellum. *Scientific Reports*, 7, p.46181.